A novel nematode species from the Siberian permafrost shares adaptive mechanisms for cryptobiotic survival with *C. elegans* dauer larva

Anastasia Shatilovich[1#], Vamshidhar R. Gade[2,9#], Martin Pippel[3], Tarja T. Hoffmeyer[4], Alexei V. Tchesunov[5], Lewis Stevens[6], Sylke Winkler[2,7], Graham M. Hughes[8], Sofia Traikov[2], Michael Hiller[3,10], Elizaveta Rivkina[1], Philipp H. Schiffer[4*], Eugene W Myers[3], Teymuras V. Kurzchalia[2*]

1. Institute of Physicochemical and Biological Problems in Soil Science RAS, Pushchino, Russia
2. Max Planck Institute for Molecular Cell Biology and Genetics, Dresden, Germany
3. Center for Systems Biology, Dresden, Germany
4. Institute for Zoology, University of Cologne
5. Department of Invertebrate Zoology, Faculty of Biology, M.V. Lomonosov Moscow State University, Moscow, Russia
6. Tree of Life, Wellcome Sanger Institute, Cambridge, UK
7. DRESDEN concept Genome Center, Dresden, Germany
8. School of Biology and Environmental Science, University College Dublin, Belfield, Dublin, Ireland
9. Institute of Biochemistry, ETH Zürich, 8093 Zürich, Switzerland
10. LOEWE Centre for Translational Biodiversity Genomics, Senckenberg Society for Nature Research & Goethe University, Frankfurt am Main, Germany

[#] A.S and V.G contributed equally to this work

*To whom correspondence may be addressed

Email: kurzchalia@mpi-cbg.de

p.schiffer@uni-koeln.de

Abstract

Some organisms in nature have developed the ability to enter a state of suspended metabolism called cryptobiosis[1] when environmental conditions are unfavorable. This state-transition requires execution of a combination of genetic and biochemical pathways[1,2,3] that enable the organism to survive for prolonged periods. Recently, nematode individuals have been reanimated from Siberian permafrost after remaining in cryptobiosis. Preliminary analysis indicates that these nematodes belong to the genera *Panagrolaimus* and *Plectus*[4]. Here, we present precise radiocarbon dating indicating that the *Panagrolaimus* individuals have remained in cryptobiosis since the late Pleistocene (~46,000 years). Phylogenetic inference based on our genome assembly and a detailed morphological analysis demonstrate that they belong to an undescribed species, which we named *Panagrolaimus n. sp*. Comparative genome analysis revealed that the molecular toolkit for cryptobiosis in *Panagrolaimus n. sp.* and in *C. elegans* is partly orthologous. We show that biochemical mechanisms employed by these two species to survive desiccation and freezing under laboratory conditions are similar. Our experimental evidence also reveals that *C. elegans* dauer larvae can remain viable for longer periods in suspended animation than previously reported. Altogether, our findings demonstrate that nematodes evolved mechanisms potentially allowing them to suspend life over geological time scales.

Introduction

Organisms from diverse taxonomic groups can survive extreme environmental conditions, such as the complete absence of water or oxygen, high temperature, freezing, or extreme salinity. The survival strategies of such organisms include a state known as suspended animation or cryptobiosis, in which they reduce metabolism to an undetectable level[6]. Spectacular examples of long-term cryptobiosis include a *Bacillus* spore that was preserved in the abdomen of bees buried in amber for 25 to 40 million years[7], and a 1000 to 1500 years-old *Lotus* seed, found in an ancient lake, that was subsequently able to germinate[8]. Metazoans such as tardigrades, rotifers and nematodes are also known for remaining in cryptobiosis for prolonged periods[9,10]. The longest records of cryptobiosis in nematodes are reported for the Antarctic species *Plectus murrayi*[11] (25.5 years in moss frozen at -20°C), and *Tylenchus polyhypnus*[12] (39 years desiccated in an herbarium specimen).

Intensive research during the last decade has demonstrated that permafrosts (perennially frozen sediments) are unique ecosystems preserving life forms at sub-zero temperatures over thousands of years[13,14,15,16]. Permafrost remains are an exceptional source for discovering a wide variety of unicellular and multicellular living organisms surviving in cryptobiosis for prolonged periods[6,17,18]. The Siberian permafrost is a unique repository for preserving organisms in sub-zero temperatures for millions of years. Expeditions in the past decade have resulted in the revival of several organisms across various taxa from the Siberian permafrost[5,36,37,38]. The possibility to exploit permafrost as a source for reanimating multicellular animals was recognized as early as 1936. A viable Cladocera crustacean *Chydorus sphaericus*, preserved in the Transbaikalian permafrost for several thousand years[39,40], was discovered by P.N. Kapterev, who worked at the scientific station Skovorodino as a GULAG prisoner. Unfortunately, this observation remained unnoticed for many decades. We recently reanimated soil nematodes that were preserved in Siberian permafrost for potentially thousands of years, and initial morphological observations provisionally described them as belonging to the genera *Panagrolaimus* and *Plectus.* Previous studies demonstrated several species of *Panagrolaimus* can undergo cryptobiosis in the form of anhydrobiosis (through desiccation) and cryobiosis (through freezing)[19,20,21,22,23]. In various nematodes, entry into anhydrobiosis is often accompanied by a preparatory phase of exposure to mild desiccation, known as preconditioning[21,24]. This induces a specific re-modelling of the transcriptome, the proteome, and metabolic pathways that enhances survival ability[2,3,25]. Some panagrolaimids possess adaptive mechanisms for rapid desiccation where most of the cellular

water is lost, while others possess freezing tolerance without loss of water at sub-zero temperatures by inhibiting the growth and recrystallisation of ice crystals[21].

Here we present a high-quality genome assembly, detailed morphological phylogenetic analysis, and define a novel species, *Panagrolaimus n. sp.* Precise radiocarbon dating indicates that *Panagrolaimus n. sp* remained in cryptobiosis for about 46,000 years, since the late Pleistocene. Furthermore, making use of the model organism *C. elegans*, we demonstrate that *C. elegans* dauer larvae and *Panagrolaimus* utilize comparable molecular mechanisms to survive extreme desiccation and freezing, i.e. upregulation of trehalose biosynthesis and gluconeogenesis.

Results

Discovery site and radiocarbon dating

Previously, we had shown that nematodes from the Siberian permafrost with morphologies consistent with the genera *Panagrolaimus* and *Plectus* could be reanimated thousands of years after they had been frozen. Several viable nematode individuals were found in two of the more than 300 studied samples of permafrost deposits spanning different ages and genesis. Samples were collected by researchers of the Soil Cryology Lab, Pushchino, Russia, during perennial paleo-ecological expeditions carried out in the coastal sector of the northeastern Arctic[17]. The detailed description of the study site (outcrop Duvanny Yar, Kolyma River, Fig.1A), sampling and revitalizing procedures are provided in Supplementary Information (SI). Like other late Pleistocene permafrost formations in the northeastern Arctic, Duvanny Yar is composed of permanently frozen ice-rich silt deposits riddled with large polygonal ice wedges that divide them into mineral blocks[26,27] (Fig.1B). Sediments include sandy alluvial layers, peat lenses, buried paleosols and Pleistocene rodent burrows (Fig.1C). The burrow (P-1320), in which *Panagrolaimus* nematodes were found (Fig.1D), has been taken from the frozen outcrop wall at a depth of about 40 m below the surface and about 11 m above river water level in undisturbed and never thawed late Pleistocene permafrost deposits. The fossil burrow left by arctic gophers of the genus *Citellus* consists of an entrance tunnel and large nesting chamber up to 25 cm in diameter[26].

The sterility of permafrost sampling and age of cultivated biota have been discussed in detail in several reviews[14,28, 29]. Based on previous reports, the age of the organisms found in a burrow is equal to the freezing time and corresponds to the age of organic matter conserved in the syncryogenic sediments. This makes it possible to use radiocarbon dating of organic matter

130 to establish the age of organisms. We performed Accelerator Mass Spectrometry (AMS)
131 radiocarbon analysis of plant material obtained from studied borrow P-1320 and determined a
132 direct ^{14}C age of 44,315±405 BP (Institute of Geography, RAS; sample $IGAN_{AMS}$ 9137).
133 Calibrated age range is 45,839 – 47,769 cal BP (95.4% probability) (Fig.S1).
134
135 **Like other parthenogenetic *Panagrolaimus*, the newly discovered species is triploid**
136 The revived animal was cultivated in the laboratory for over 100 generations and initially
137 described as *Panagrolaimus* aff. *detritophagus*[4] based on morphology. We conducted a
138 detailed morphological analysis of the revived animal (Fig.2, S2, Table S1; BOX1), which
139 confirmed unambiguously that the animal belongs to the genus of *Panagrolaimus*, in
140 agreement with a previous phylogenetic analysis of the 18S ribosomal RNA sequence[4].
141 However, due to the morphological uniformity of *Panagrolaimus*, unusual even for nematodes,
142 morphology and molecular analysis of a single ribosomal RNA sequence is insufficient to
143 describe a species. We found the species to be parthenogenetic, which further complicates
144 description under most species concept. Due to these limitations, we decided to refer to the
145 phylogenetic species concept, using phylogenetic trees based on multiple genes as markers.
146 To obtain comprehensive molecular data for phylogenomic species determination, we
147 generated a genome assembly usinging PacBio HiFi sequencing with long reads (84X
148 coverage, mean length 14,425 bp). Our analysis of repeat and gene content is described in
149 Supplementary Table 3. K-mer analysis of the reads clearly indicated that this animal has a
150 triploid genome (Fig.3A), like other parthenogenetic *Panagrolaimus* species[30]. Despite the
151 challenges that a triploid genome poses for assembly, we obtained a highly contiguous contig
152 assembly of the three pseudohaplotypes that comprise almost 266 Mb and thus have a similar
153 genome size as other parthenogenetic *Panagrolaimus* species[30]. The contig N50 value of all
154 three pseudohaplotypes is 3.8 Mb. Since these pseudohaplotypes exhibited a noticeable degree
155 of divergence, we further investigated their relationship by using the apparent homeologs in
156 our gene predictions to align the longest continuous contigs based on micro synteny (Fig. 3B).
157 Links between the contigs clearly show the triploid state of the genome.
158
159
160
161
162

163 **BOX 1 Description of *Panagrolaimus n. sp* sp. nov.**

Description	Body spindle-shaped and usually almost straight after fixation (Fig.2a, b). Cuticle thin and faintly annulated, 10–11 annules per 10 µm in cervical region, 13–14 in midbody, preanally again 10 annules within 10 µm. Conspicuous convex lateral fields with three incisures 1.5-2 µm wide extended along the body from about ¼–1/3 procorpus length to 2/3 of tail length. In SEM, the lateral field looks like a bolster with a narrow median split. Labial region set off. Mouth opening surrounded with six lips (Fig.2c, d). Anterior sensilla as papillae arranged in two close but separate subsequent circles. Somatic sensilla (i.e., deirids and phasmids) not evident. Buccal cavity cylindro-conoid, and unarmed; its total length 9–13 µm, maximum stoma width 1.7–2.8 µm (Fig.2e). Dorsal stoma wall (dorsal rhabdion) more clearly sclerotized. Anterior part of the buccal cavity comprising cheilostom and gymnostom nearly cylindroids while stegostom conically narrowed and ended with a distinct tight flexion. Pharynx consists of three distinct parts: straight anterior procorpus, narrow medial isthmus and rounded terminal bulb. Procorpus gradually widening to it posterior end, always straight in all specimens, with transversal muscular striation, more prominent in posterior three fourths. Isthmus narrow, cylindroid, bent starkly in nearly all studied specimens. Terminal bulb strongly muscular, with a valvular apparatus at about 40% of the bulb length. Cardia in shape of truncate cone. Intestine (midgut) tissue filled with vacuoles and granules; in the anteriormost region, the granules smaller and look more pallid. Cell borders not visible in the intestine, but internal lumen distinct, sinusoid. No internal content visible in the internal lumen. Ventral excretory-secretory pore and its cuticularized duct situated at the level of anterior part of the bulb. No other details of the excretory-secretory system visible. Vulval lips protruding. Genital branch monodelphic prodelphic and situated dorsally and to the right of the midgut (Fig.2f). Vagina distinctly cuticularized and opens to the elongate uterus. A long oviduct extended anteriad from the anterior uterus; the oviduct folded up and then posteriorward and transforms into an elongate ovary. There are

	one or two ripe eggs in the uterus in most specimens. Tail short conical, with short acute spike-like mucro (Fig.2g).
Etymology	Species name *kolymaensis* (Latin) is derived from the Kolyma River area.
Holotype	Senckenberg Natural History Museum, Frankfurt am Main, Germany (collection number SMF 17067).
Paratypes	Senckenberg Natural History Museum, Frankfurt am Main, Germany (collection numbers SMF 17068, SMF 17069) (eighteen paratypes).
Type locality	Frozen fossil rodent burrow buried in permafrost 45,839 – 47,769 cal BP, 40 meters from the surface, outcrop Duvanny yar, Kolyma River, North-East of Siberia, Russia (68.633410, 159.078800). Frozen material from burrow was collected by Dr.S.Gubin (Soil Cryology Lab, Pushchino, Russia) in august 2002.

Applying a phylogenomic concept to define *Panagrolaimus n. sp* sp. nov.

To place the species in the genus *Panagrolaimus*, we conducted a broader multi-gene phylogenomic analysis using Maximum likelihood methods. Our analysis of a concatenated, partitioned alignment of 60 genes, and a coalescence-based approach using a broader set of 12,295 gene trees, retrieves the revived animal as sister to all other sequenced *Panagrolaimus* species, but as an ingroup to *Propanagrolaimus*[31] (Fig.3C; Fig. S3B-C). Thus, the phylogenetic placement provides strong evidence that this animal represents a novel species. Furthermore, there is substantial sequence divergence between this novel species, and *Panagrolaimus* sp. PS1159 and *Panagrolaimus* sp. ES5, estimated to be on average 2.06 and 2.11 amino acid substitutions per site in our concatenated alignment, respectively. The substantial divergence is in line with previous data on ages of *Panagrolaimus* nematodes[30], and more broadly seen in nematodes, which can be hyper-diverse[32,33]. Our data also contradicts the assumption that parthenogenesis is a monophyletic trait[30] in the *Panagrolaimus* genus (Fig.3C). Using the gene-tree reconciliation approach implemented in GRAMPA (Gene-tree Reconciliation Algorithm with MUL (Multi labelled)-trees for Polyploid Analysis), we explored whether the additional set of proteins we found in the parthenogenetic species is a result of auto- or allopolyploidy. Finding these the additional proteins basally branching, outside of the lineage containing both

182 parthenogenetic and sexual species, suggests that an allopolyploid origin of these extra gene
183 copies (Fig.S6). Based on the Kolyma River location where the animal was unearthed, we
184 propose the following taxonomic classification and species name:
185 Phylum Nematoda Potts, 1932
186 Class Chromadorea Inglis 1983
187 Suborder Tylenchina Thorne, 1949
188 Family Panagrolaimidae Thorne, 1937
189 *Panagrolaimus* sp. nov.
190

191 **_C. elegans_ dauer larvae and _Panagrolaimus n. sp._ might utilize partially similar**
192 **mechanisms to enter and remain in cryptobiotic state for prolonged periods of time**

193 In the absence of established genetic methods in *Panagrolaimus n. sp.*, we referred to
194 the model *C. elegans* as a comparator system to gain insights into possible pathways for long
195 term survival[3,4,24,25]. The high-quality genome of *Panagrolaimus n. sp.* allowed us to compare
196 its molecular toolkit for cryptobiosis with that of *C. elegans*. We used orthology clustering and
197 phylogenetics to investigate whether the genome of *Panagrolaimus n. sp.* contains genes
198 previously implicated in cryptobiosis in the *C. elegans* dauer larva. Our analysis showed that,
199 like other *Panagrolaimus* species[34,35], *Panagrolaimus n. sp.* also encodes orthologs to a *C.*
200 *elegans* trehalose phosphate synthase gene (*tps-2*) and to a trehalose phosphatase gene (*gob-1*)
201 (Fig. 3D, supplementary file Orthology analysis). Furthermore, we found orthologs to all *C.*
202 *elegans* enzymes required for polyamine biosynthesis, the TCA cycle, glycolysis,
203 gluconeogenesis, and glyoxylate shunt (Fig.3D, supplementary file Orthology analysis)
204 suggesting that *Panagrolaimus n. sp.* might partially utilize similar molecular mechanisms as
205 *C. elegans* to facilitate survival of unfavorable conditions.

206 Our earlier findings established that amongst several developmental stages of *C.*
207 *elegans*, only the dauer larva, formed during unfavorable conditions (such as low nutrients and
208 high population density), could survive anhydrobiosis and exposure to freezing[4,24]. The dauer
209 larvae is in a hypometabolic state with distinct metabolic properties such as reduced oxygen
210 consumption and heat dissipation in comparison to other larval stages of *C. elegans*. To survive
211 extreme desiccation, *C. elegans* dauer larvae (in its hypometabolic state) need to be first
212 preconditioned at high relative humidity (98% RH) for 4 days[24]. During preconditioning, dauer
213 larvae upregulate trehalose biosynthesis that ensures their survival to harsh desiccation[24,25]. We
214 tested whether survival of *Panagrolaimus n. sp.* is also facilitated by preconditioning. As there

215 is no dauer stage in the *Panagrolaimus* life cycle, we performed our experiments with a
216 population of all the larval stages and adults. Although a small proportion of *Panagrolaimus*
217 *n. sp.* individuals survive harsh desiccation and freezing without preconditioning (Fig.4A), the
218 mixture of all the larval stages and adults of *Panagrolaimus n. sp.* survive significantly higher
219 (p value< 0.0001) in proportion to harsh desiccation upon preconditioning (Fig.4A). Similarly,
220 preconditioning and desiccation further enhanced survival rate of *Panagrolaimus n. sp.* to
221 freezing (-80°C) (Fig.4A). Like *C. elegans* dauer larva, *Panagrolaimus n. sp.* upregulates
222 trehalose levels up to 20-fold upon preconditioning (Fig.4B). We previously reported that, to
223 upregulate trehalose levels upon preconditioning, *C. elegans* dauer larva dissipate their fat
224 reserves (Triacylglycerols) by activating the glyoxylate shunt and gluconeogenic pathway[25].
225 Upon preconditioning, we found that triacylglyceride (TAG) levels are significantly decreased
226 in *Panagrolaimus n. sp.* (Fig.S5A&B). To further investigate whether acetyl-CoA derived from
227 the degradation of TAGs culminates in trehalose, we applied the previously developed method
228 of metabolic labelling with ^{14}C-acetate in combination with 2D-TLC [4,25]. The ^{14}C-acetate
229 metabolized by the worms is incorporated into TAGs. Upon degradation of TAGs, ^{14}C-acetyl
230 CoA is released which acts as a precursor for trehalose biosynthesis. As shown in Fig. 4C,
231 preconditioning led to a huge increase of radioactivity in trehalose and to a small increase in
232 some amino acids (glycine/serine, phenylalanine; panels c and d). Interestingly,
233 *Panagrolaimus n. sp.* displayed an additional spot (Fig. 4D, enumerated as 7), that was not
234 found in *C. elegans*. We identified this spot as trehalose-6-phosphate (Fig.S5C-H), a precursor
235 of trehalose, based on the fragmentation pattern of the molecule, using mass spectrometry.
236 Thus, to resist harsh desiccation, like *C. elegans* dauer larvae, *Panagrolaimus n. sp.* might
237 utilize the glyoxylate shunt and consequently acetate derived from TAGs to synthesize
238 trehalose. Detection of the immediate precursor (trehalose-6-phosphate) suggests that the flux
239 of metabolites is intense in *Panagrolaimus n. sp*. Finally, we investigated whether *C. elegans*
240 dauer larvae can also survive in prolonged cryptobiotic state. Despite preconditioning, the
241 survival ability of desiccated dauer larvae at room temperature declines very rapidly, with most
242 larvae dead after almost 10 days (Fig. 4E) (Fig. S4A&B). Direct freezing without any
243 cryoprotectants at -80℃ leads to instant death of the animals. To test whether combining these
244 conditions could extend the viability of dauer larvae (Fig. S4A&B), we transferred the
245 desiccated larvae to -80℃. Remarkably, under these conditions, there was no significant
246 decline in viability even after 480 days (Fig. 4E). Moreover, after thawing the animals resumed
247 reproductive growth and produced progeny in numbers like those of animals kept under control

conditions (Fig. 4F). Since we did not observe any reduction in the survival at any time points, this suggests that the combination of anhydrobiosis and freezing can prolong the survival ability of dauer larvae. Thus, *C. elegans* dauer larvae, when exposed to combination of cryptobiotic states can survive for extremely long periods of time.

Discussion

The new nematode species from permafrost can now be placed into the genus *Panagrolaimus*[41], which contains several described parthenogenetic and gonochoristic species[30,42]. Many *Panagrolaimus* display adaptation to survival in harsh environments[21] and the genus includes the Antarctic species *P. davidi*[22]. The genus *Panagrolaimus* is exceptional in its morphological uniformity even among nematode species that are hard to classify based on morphology in general. Thus, species designation via microscopic (including SEM) analysis is unreliable, which is further complicated by the absence of males in parthenogenetic species. Males have an important diagnostic feature such as spicules and pericloacal papillae, females differ from one species to another mainly by morphometrics, where interspecies differences (absolute measures and ratios) might be subtle. Our specimens are similar based on absolute sizes and ratios to females of the bisexual species *Panagrolaimus detritophagus*[43]. The only non-overlapping morphometric character is index "b" (body length: pharynx length): 5.6–6.8 in *Panagrolaimus n. sp.* versus 4.4-5.1 in *P. detritophagus*.

Consequently, we turned to phylogenomic methods under the phylogenetic species concept to place the species on the tree. This showed that this species is an outgroup to other known *Panagrolaimus* species, raising the possibility of a second independent evolution of parthenogenesis in the genus, in contrast to previous findings[42,31,30]. Alternatively, the hybrid origin of parthenogenetic *Panagrolaimus* could influence the phylogenetic positioning of strains, raising the possibility that the new species is a true sister to the other parthenogenetic strains. To fully resolve the phylogenetic positioning further, extensive sampling, and genome sequencing of *Panagrolaimus* species is needed. We found *Panagrolaimus n. sp.* to be triploid and thus a hybrid origin is possible, as seen in other parthenogenetic *Pangrolaimus*[30]. The highly contiguous genome of *Panagrolaimus n. sp.* will allow for analyses of this trait in comparison to other *Panagrolaimus* species currently being genome sequenced.

Our results provide a deeper insight into the homology of molecular and biochemical mechanisms between *C. elegans* and *P. kolymaensis*, which are not only taxonomically but also ecologically distinct. *C. elegans* can mostly be found in rotting fruits and plants in

281 temperate regions[44,45], while *Panagrolaimus* species are globally distributed and prevalent in
282 leaf litter and soil[42], including in harsh environments[21]. We show through orthology analysis
283 that the well-studied molecular pathways used by *C. elegans* larvae to enter the dauer state,
284 such as insulin[46,47] (DAF-11, DAF-2 & DAF-16), TGF-β[48] (DAF-7), steroid[49] (DAF-9, DAF-
285 12) are present in the genome of the *Panagrolaimus n. sp.* (Fig.S4C). The presence of
286 homologous genes in two species does not necessarily demonstrate their functionality in both.
287 Therefore, further functional analyses are needed to study molecular pathways in detail.
288 Trehalose accumulation (Fig.4B) and depletion of triacylglycerols (Fig.S5A&B) ensures the
289 functionality of trehalose biosynthesis pathway and utilization of glyoxylate shunt during
290 desiccation in *Panagrolaimus n. sp.* Without the activity of the enzyme TPS-2 and glyoxylate
291 shunt, it is unfeasible to synthesize trehalose in nematodes. We do not eliminate the possibility
292 of other biochemical features that might contribute to desiccation survival ability of
293 *Panagrolaimus n. sp*, but with regards to trehalose biosynthesis and the glyoxylate shunt, our
294 data suggest that molecular tool kit is partially orthologous. In our future studies, we intend to
295 perform RNAi based experiments to infer the concrete mechanisms. Our results hint at
296 convergence or parallelism in the molecular mechanisms organizing dauer formation and
297 cryptobiosis.

298 As mentioned above, preconditioning enhances the survival of *Panagrolaimus n. sp*.
299 by rendering them desiccation tolerant. We previously reported that preconditioning elevates
300 trehalose biosynthesis in *C. elegans* dauer larvae and the elevated trehalose renders desiccation
301 tolerance by protecting the cellular membranes[24]. It is not surprising that *Panagrolaimus n. sp.*
302 upregulates trehalose, however the magnitude of trehalose elevation is higher than *C. elegans*
303 dauer larvae. This indicates that central regulators (DAF-16, DAF-12) of trehalose
304 upregulation may differentially regulate *tps-2* in *Panagrolaimus n. sp*[50,51,34]. Although
305 *Panagrolaimus n. sp.* utilizes the glyoxylate shunt and gluconeogenesis to upregulate trehalose
306 levels, it is intriguing to observe that they accumulate substantial levels of trehalose-6-
307 phosphate. Further investigation of this observation using RNAi or inhibitor-based experiments
308 will provide insights into molecular mechanisms of metabolic regulation in *Panagrolaimus n.*
309 *sp.* upon preconditioning. Our findings for the first time demonstrate that *C. elegans* dauer
310 larvae possess an inherent ability to survive freezing for prolonged periods if they undergo
311 anhydrobiosis. It is tempting to speculate that undergoing anhydrobiosis might be a survival
312 strategy of *C. elegans* to survive the seasonal changes in nature.

In summary our findings indicate that by adapting to survive cryptobiotic state for short time frames in environments like permafrost, some nematode species gained the potential for individual worms to remain in the state for geological timeframes. This raises the question whether there is an upper limit to the length of time an individual can remain in the cryptobiotic state. Long timespans may be limited only by drastic changes to the environment such as strong fluctuations in ambient temperature, natural radioactivity, or other abiotic factors. These findings have implications for our understanding of evolutionary processes, as generation times may be stretched from days to millennia, and long-term survival of individuals of species can lead to the refoundation of otherwise extinct lineages. This is particularly interesting in the case of parthenogenetic species, as each individual can found a new population without the need for mate finding, i.e. evading the cost of sex. Finally, understanding the precise mechanisms of long-term cryptobiosis and cues that lead to successful revivals can inform new methods for long term storage of cells and tissues.

Methods

Materials and *C. elegans* strains

[1-14C] -acetate (sodium salt) was purchased from Hartmann Analytic (Braunschweig, Germany). All other chemicals were purchased from Sigma-Aldrich (Taufkirchen, Germany). The *Caenorhabditis* Genetic Centre (CGC) which is funded by NIH Office of Research Infrastructure Programs (P40 OD010440) provided *daf-2(e1370)* and *E. coli NA22* strains.

Genomic DNA isolation from *Panagrolaimus n. sp* nematodes

After isolation (Supplementary Information), to ensure our strain *Panagrolaimus n. sp.* (Pn2-1) can adapt to different laboratories, we grew them for multiple generations. The strain was in culture for several generations during genomic DNA isolation and was frozen after genomic DNA isolation was performed. *Panagrolaimus n. sp.* nematodes (isofemale strain Pn2-1) were grown on several plates of NGM agar plated with *E. coli NA22* bacteria at 20°C. Worms were collected from the plates, washed with water at least three to five times by centrifugation at 1000 g to remove any residual bacteria and any debris. The worm pellet was dissolved in 5 volumes of worm lysis buffer (0.1M Tris-HCl pH=8.5, 0.1M NaCl, 50mM EDTA pH=8.0) and distributed in 1.5 ml of microcentrifuge tubes. These tubes are incubated at -80°C for 20 minutes. 100 µl of Proteinase 'K' (20 mg/ml) was added to each tube and they are incubated at 60°C overnight. 625 µl of cold GTC buffer (4M Guanidinium Thiocynate, 25mM Sodium citrate, 0.5% (v\v) N-lauroylsarcosine, 7%(v/v) Beta Mercaptoethanol) was added to the tube, incubated on ice 30 min, and mixed by inverting every 10 min. 1 volume of phenol–chloroform-isoamyl alcohol (pH=8) was added to the lysate and mixed by inverting the tube 10-15 times. Tubes were centrifuged for 5 min at 10,000 g at 4°C to separate the phases. The upper aqueous phase was carefully collected into a fresh tube. One volume of fresh chloroform was added and mixed by inverting the tubes for 10-15 times and centrifuged for 5 min at 10,000 g at 4°C to separate the phases. One volume of cold 5 M NaCl was added, mixed by inverting the tubes and incubated on ice for 15 min. After incubation these tubes were centrifuged for 15 min at 12,000–16,000 g at 4°C. The supernatant containing the nucleic acids were slowly transferred into a fresh tube. One volume of isopropanol was added to the tube, inverted few times, and incubated on ice for 30 minutes. After incubation, the tubes were centrifuged at 3000 g for 30–45 min at 25°C and the supernatant was discarded without disturbing the pellet. The pellet was washed twice with 1 ml of 70% ethanol, tubes were centrifuged at 3000 g for 5 min and supernatant was discarded and incubated at 37°C for 10-15 min to dry the pellet. The

359 pellet was resuspended carefully in TE buffer. The quality of the genomic DNA was analyzed
360 with pulse field gel electrophoresis.
361
362 **Genome sequencing and assembly**
363 The long insert library was prepared as recommended by Pacific Biosciences according to the
364 'Procedure & Checklist-Preparing gDNA Libraries Using the SMRTbell® Express Template
365 Preparation Kit 2.0' protocol. In summary, RNAse treated HMW gDNA was sheared to 20 kb
366 fragments on the MegaRuptor™ device (Diagenode) and 10 µg sheared gDNA was used for
367 library preparation. The PacBio SMRTbell™ library was size selected in two fractions (9-
368 13kb, > 13kb) using the BluePippin™ device with cassette definition of 0.75% DF MarkerS1
369 3-10 kb Improved Recovery. The second fraction of the size-selected library was loaded with
370 95 *p*M on plate on a Sequel SMRT cell (8M). Sequel polymerase 2.0 was used in combination
371 with the v2 PacBio sequencing primer and the Sequel sequencing kit 2.0EA, with a runtime of
372 30 hours. We created PacBio CCS reads from the subreads .bam file using PacBio's ccs
373 command linetool (version4.2.0), outputting 8.5Gb of high-quality CCS reads (HiFi reads N50
374 of 14.4 kb). HiCanu (version 2.2)[39] was used to create the contig assembly. Blobtools[53] (version
375 1.1.1) was used to identify and remove bacterial contigs. The final triploid contig assembly
376 consists of 856 contigs has a N50 of 3.82 Mb and a size of 266Mb. The mitochondrial genome
377 was created with the mitoHifi pipeline (version 2, https://github.com/marcelauliano/MitoHiFi)
378 based on the assembled contigs and the closely related reference mitochondrial genome of
379 *Panagrellus redivivus* (strain: PS2298/MT8872, ENAaccession: AP017464). The mitoHifi
380 pipeline identified 49 mitochondrial contigs ranging from 13-32Kb. The final annotated
381 circular mitochondrial genome has a length of 17467 bp.
382 To identify pseudohaplotypes in the *Panagrolaimus n. sp.* genome assembly, we
383 selected the longest isoform of each predicted protein-coding gene in our assembly and in the
384 *C. elegans* genome (downloaded from WormBase Parasite, release WBPS15) using AGAT
385 (version 0.4.0) and clustered them into orthologous groups (OGs) using OrthoFinder (version
386 2.5.2). We identified OGs that contained three *Panagrolaimus* sequences (i.e. groups that were
387 present as single-copy in all three pseudohaplotypes) and used these to identify trios of multi-
388 megabase size contigs derived from the three pseudohaplotypes. Synteny between the three
389 pseudohaplotypes was visualized using Circos to plot the positions of each homeolog (version
390 0.69-8).
391

392 **Genome annotation**

393 RepeatModeler 1.0.8 (http://www.repeatmasker.org/) was used with parameter '-engine ncbi'
394 to create a library of repeat families which was used with RepeatMasker 4.0.9 to soft-mask the
395 *Panagrolaimus* genome. To annotate genes, we cross mapped protein models from an existing
396 *Panagrolaimus* as external evidence in the Augustus based pipeline. The completeness of our
397 predictions was evaluated using BUSCO on the gVolante web interface.

398

399 **Orthology analysis**

400 We conducted a gene orthology analysis using genomic data from *Panagrolaimus n. sp*, the
401 Plectid nematode species from the permafrost, as well as genomic data from WormBase
402 Parasite (https://parasite.wormbase.org; accessed 17/12/2020): *Caenorhabditis elegans*,
403 *Diploscapter coronatus*, *Diploscapter pachys*, *Halicephalobus mephisto*, *Panagrellus*
404 *redivivus*, *Panagrolaimus davidi*, *Panagrolaimus* sp. ES5, *Panagrolaimus* sp. PS1159,
405 *Panagrolaimus superbus*, *Plectus sambesii*, and *Propanagrolaimus* sp. JU765. For plectids,
406 genomic resources are scarce. We therefore added transcriptome data of *Plectus murrayi*,
407 *Anaplectus granulosus*, *Neocamacolaimus parasiticus*, and *Stephanolaimus elegans*, with the
408 latter three transcriptomes kindly provided by Dr. Oleksandr Holovachov (Swedish museum
409 of natural history). Transcriptomes for *Anaplectus granulosus*, and *Neocamacolaimus*
410 *parasiticus* have been published and are readily available [55,56]. All three transcriptomes were
411 assembled *de novo* with Trinity[57]. The exact procedures are described in the respective
412 publications[55,56]. The *Stephanolaimus elegans* transcriptome was assembled using the same
413 methodologies as *Neocamacolaimus parasiticus*.

414 The *Plectus murrayi* transcriptome was built from raw reads deposited at NCBI
415 (https://sra-downloadb.be-md.ncbi.nlm.nih.gov/sos2/sra-pub-run-
416 13/SRR6827978/SRR6827978.1; accessed 22.12.2020) and assembled using Galaxy Trinity
417 version 2.9.1[58], [57]. All default options were used including *in silico* normalization of reads
418 before assembly. Transdecoder (conda version 5.5.0)[59] was used to translate to amino acid
419 sequence. Identical reads were removed with cd-hit version 4.8.1[60,61], with shorter isoforms
420 removed using the Trinity get_longest_isoform_seq_per_trinity_gene.pl command[59] (Trinity
421 conda version 2.8.5; Anaconda Software Distribution, Conda, Version 4.9.2, Anaconda, Nov.
422 2020). Amino acid translations of the longest isoforms were extracted with AGAT (Dainat,
423 https://www.doi.org/10.5281/zenodo.3552717) from genome assembly FASTA files and
424 genome annotation GFF3 files using the 'agat_convert_sp_gxf2gxf.pl',

425 'agat_sp_keep_longest_isoform.pl' and 'agat_sp_extract_sequences.pl' scripts, respectively.
426 All FASTA headers were modified to allow for simple species assignment of each sequence in
427 subsequent analysis. Orthology analysis was conducted with OrthoFinder v. 2.5.1[62,63] using
428 default settings. For genes of interest, we constructed alignments with MAFFT v. 7.475[64] using
429 the localpair and maxiterate (1000) functions. Spurious sequences and areas that were not well
430 aligned were removed with Trimal v. 1.4.rev22[65] (procedure stated in supplementary file
431 Orthology analysis below each phylogeny). We then ran phylogenetic analysis with Iqtree2 v.
432 2.0.6[66], with -bb 1000 option, testing the model for each analysis (models eventually used
433 stated in supplementary file Orthology analysis). PFAM domains were explored using
434 Interproscan v. 5.50-84.0[67]. The phylogenies were visualized with Dendroscope 3.7.6[68] and
435 figures were created with Inkscape (https://inkscape.org). The majority of our analysis was
436 performed on the HPC RRZK CHEOPS of the Regional Computing Centre (RRZK) of the
437 University of Cologne.
438
439 **Phylogenomics**
440 Sequences of 18S and 28S genes from 44 taxa across the *Propanagrolaimus*, *Panagrolaimus*,
441 *Panagrellus* and *Halicephalobus* genera (all listed in Supplementary information) were aligned
442 (MAFFT L-INS-I v7.475)[64], concatenated [69]and used to infer a species tree using maximum
443 likelihood via (IQTREE)[70] and partitioned by best-fit models of sequence evolution for both[71].
444 Nodal support was determined using 1000 bootstrap pseudoreplicates. A further 60 genes from
445 101 taxa (all listed in Supplementary information) were used to confirm the taxonomic position
446 using the supermatrix concatenation methods outlined above. Given the limitations of
447 differential gene sampling, we expanded our phylogenomic analyses to include a coalescence
448 approach using 12,295 ML gene trees inferred for orthogroups containing the target animal.
449 Instances of multiple genes per species per group were treated as paralogs/orthologs and
450 analysed using ASTRAL-Pro[72]. Given the number of copies of genes per orthogroup, we
451 explored whether auto or alloploidy was the source of extra genes observed using the gene-tree
452 reconciliation approach implemented in GRAMPA (Gene-tree Reconciliation Algorithm with
453 MUL (Multi labelled)-trees for Polyploid Analysis)[75]. All gene trees rooted at the midpoint and
454 the final ASTRAL-pro species tree were used as inputs, with the most parsimonious result
455 analyzed further.
456
457

458 **Desiccation survival assay**

459 *C. elegans* dauer larvae desiccation assays were performed as described in[24]. *Panagrolaimus*
460 *n. sp* desiccation assays were performed similarly as described in[24] with mixed population
461 (Mixture of all larval stages and adults) of the nematodes.

462

463 **Exposure of nematodes to extreme environments**

464 *C. elegans* dauer larvae or mixed population (Mixture of all larval stages and adults) of
465 *Panagrolaimus n. sp* nematodes were preconditioned and desiccated as described in[24], then
466 transferred to elevated temperature of 34°C, freezing (-80°C) and anoxia. Anoxic environment
467 was generated in a desiccation chamber at 60%RH by flushing the Nitrogen gas into the
468 chamber. The concentration of oxygen inside the chamber was monitored. After each timepoint
469 they were rehydrated with 500 µl of water for 2-3 hours. Rehydrated worms were transferred
470 to NGM agar plates with *E. Coli NA22* as food. Survivors were counted after overnight
471 incubation at 15°C. Each experiment was performed on two different days with at least two
472 technical replicates.

473

474 **Trehalose quantification from nematode lysates**

475 Trehalose measurements were performed as described in previous reports[25].

476

477 **Radiolabeling, metabolite extraction and 2D-TLC**

478 The above-mentioned procedures were performed according to previous reports[3,25].

479 **Identification of trehalose-6-phosphate from TLC plates**

480 Normalized aqueous fractions from the non-preconditioned and preconditioned samples were
481 separated by high performance thin layer chromatography (HPTLC), using 1-propanol-
482 methanol-ammonia (32%)-water (28:8:7:7 v/v/v/v) as first, dried for 15 min and 1-butanol-
483 acetone-glacial acetic acid–water (35:35:7:23 v/v/v/v) second dimension respectively. Using
484 the trehalose as a standard on both dimensions of the TLC, the regions of interest were scrapped
485 out from the TLCs. The scraped-out silica was extracted with 10 ml of 50% methanol twice.
486 The fractions were combined, dried under vacuum and dissolved in 100 µl of MS mix solution
487 containing 4:2:1 (Isopropanol:Methanol:Chloroform) with 7.5 mM ammonium formate. Mass
488 spectrometric analysis was performed on a Q Exactive instrument (Thermo Fischer Scientific,
489 Bremen, DE) equipped with a robotic nanoflow ion source TriVersa NanoMate (Advion
490 BioSciences, Ithaca, USA) using nanoelectrospray chips with a diameter of 4.1 µm. The ion

491 source was controlled by the Chipsoft 8.3.1 software (Advion BioSciences). Ionization voltage
492 was + 0.96 kV in negative mode; backpressure was set at 1.25 psi. The temperature of the ion
493 transfer capillary was 200°C; S-lens RF level was set to 50%. FT MS spectra were acquired
494 within the range of m/z 50–750 at the mass resolution of R m/z 200 = 140000; automated gain
495 control (AGC) of 3×10^6 and with the maximal injection time of 3000 ms. FT MS/MS spectra
496 were acquired within the range of m/z 50–750 at the mass resolution of R m/z 200 = 140000;
497 automated gain control (AGC) of 3×10^4 and with a maximal injection time of 30 s.
498
499 **Triacylglycerols measurement from *Panagrolaimus n. sp* lysates**
500 Non-preconditioned and preconditioned pellets were lysed in 200 µl of isopropanol with 0.5
501 mm Zircornium beads twice for 15 min. The lysates were centrifuged at 1300 g for 5 min. The
502 supernatant was carefully collected without any debris, 20 µl of the lysate was used for protein
503 estimation. Normalization was performed according to soluble protein levels, supernatant
504 volumes corresponding to 50-100 µg of proteins were dried in the desiccator. 700 µl of IS
505 ((10:3 (Methyl tert-butyl ether: ethanol)) mix (warmed to room temperature) was added to
506 dried samples and left on the shaker for 1 hour. The samples were centrifuged at 1400 rpm and
507 4°C. 140 µl of water was added and left on the shaker for 15 min. These samples were
508 centrifuged at 13400 rpm for 15 min. The upper organic fraction was collected and transferred
509 to 1.5 ml glass vial and left for drying in the desiccator. The dried samples were reconstituted
510 in a volume of 300 µl of 4:2:1 (Isopropanol:Methanol:Chloroform). Volume corresponding to
511 1 µg was used for injection.
512 LC-MS/MS analysis was performed on a high-performance liquid chromatography
513 system (Agilent 1200 HPLC) coupled to a Xevo G2-S QTof (Waters). The samples were
514 resolved on a reverse phase C18 column (Cortecs C18 2.7um from Waters) with
515 50:50:0.1:1% (Water:Methanol:Formicacid:1MAmmoniumformate) and 25:85:0.1:1%
516 (Acetonitrile:Isopropanol:Formic acid:1M Ammonium formate) as mobile phase. The
517 following gradient program was used: Eluent B from 0 % to 100 % within 12 min; 100 % from
518 12 min to 17min; 0 % from 17 min to 25 min. The flow rate was set at 0.3 ml/min. The samples
519 were normalised according to the total protein concentration and the worm numbers. TAG
520 50:00:00 was used as internal standard. Skylinesoftware
521 (https://skyline.ms/project/home/software/Skyline/begin.view) was used to analyse the raw
522 data. TAGs were extracted from Lipidmaps (https://www.lipidmaps.org/) database.
523

524 **Author contributions**

525 AS, VG, PS, TK conceived and designed the study. AS, VG, TH, MP, AT, GH, MH, ER, PS
526 and TK contributed to the original draft. AS performed cultivation of nematodes, provided
527 samples for scanning electron microscopy and radiocarbon dating. VG performed desiccation
528 survival assays, trehalose measurement, 2D-TLC of metabolites, trehalose-6-phosphate
529 detection, combination of cryptobiosis experiments, genomic DNA isolation from
530 *Panagrolaimus n. sp.*, assembled the data from all the authors, prepared the figures, revised,
531 and submitted the manuscript. MP performed genome assembly. TH conducted orthology
532 analyses and single gene phylogenies and contributed to figures. AT provided morphological
533 description, light, and scanning electron microscopy. LS analyzed the genome assembly and
534 created figures. GMH performed the phylogenetic, MUL analyses and proofread the
535 manuscript. ST performed triacylglycerols measurements, trehalose-6-phosphate detection
536 with suggestions from Andrej Shevchenko. MH annotated supplementary table 3. PS performed
537 genome annotation and supervised TH and LS. EWM supervised MP and had overall
538 responsibility for sequencing and assembly including funding it.
539
540
541
542
543
544
545
546
547
548
549
550
551
552
553
554
555

Acknowledgements

VG is thankful to Andrej Shevchenko, members of Kurzchalia lab for helpful discussions and the core facilities of MPI-CBG for assistance. We are grateful to Dr. S. Gubin for field study and sampling, our colleagues in Soil Cryology Lab, Pushchino and North-East Scientific Station in Chersky, Republic of Sakha (Yakutia) for their help and cooperation. The authors thank Long Read Team of the DRESDEN-concept Genome Center, DFG NGS Competence Center, part of the Center for Molecular and Cellular Bioengineering (CMCB), Technische Universität Dresden and MPI-CBG. GMH is funded by a UCD Ad Astra Fellowship. This work was supported by the Russian Foundation for Basic Research (19-29-05003-mk) to AS and ER. VG and TK acknowledge the financial support from the Volkswagen Foundation (Life? research grant 92847). PS and TH are supported by a DFG ENP grant to PS (DFG project 434028868). The authors are thankful to Richard Roy and Jens Bast for critical reading the manuscript. We thank Iain Pattern for suggestions on writing the manuscript. The funders have no role in the design of the study.

Conflict of interest:

The authors declare they have no conflict of interest relating to the content of this article.

References

1. Hibshman, J. D., Clegg, J. S. & Goldstein, B. Mechanisms of Desiccation Tolerance: Themes and Variations in Brine Shrimp, Roundworms, and Tardigrades. *Front. Physiol.* **11**, 592016 (2020).
2. Erkut, C. *et al.* Molecular Strategies of the Caenorhabditis elegans Dauer Larva to Survive Extreme Desiccation. *PLoS ONE* **8**, e82473 (2013).
3. Gade, V. R., Traikov, S., Oertel, J., Fahmy, K. & Kurzchalia, T. V. C. elegans possess a general program to enter cryptobiosis that allows dauer larvae to survive different kinds of abiotic stress. *Sci. Rep.* **10**, 13466 (2020).
4. Shatilovich, A. V. *et al.* Viable Nematodes from Late Pleistocene Permafrost of the Kolyma River Lowland. *Dokl. Biol. Sci.* **480**, 100–102 (2018).
5. Shmakova, L. *et al.* A living bdelloid rotifer from 24,000-year-old Arctic permafrost. *Curr. Biol.* **31**, R712–R713 (2021).
6. Keilin, D. The Leeuwenhoek Lecture - The problem of anabiosis or latent life: history and current concept. *Proc. R. Soc. Lond. Ser. B - Biol. Sci.* **150**, 149–191 (1959).
7. Cano, R. & Borucki, M. Revival and identification of bacterial spores in 25- to 40-million-year-old Dominican amber. *Science* **268**, 1060–1064 (1995).
8. Shen-Miller, J. Sacred lotus, the long-living fruits of China Antique. *Seed Sci. Res.* **12**, 131–143 (2002).
9. Guidetti, R. & Jönsson, K. I. Long-term anhydrobiotic survival in semi-terrestrial micrometazoans. *J. Zool.* **257**, 181–187 (2002).
10. Tsujimoto, M., Imura, S. & Kanda, H. Recovery and reproduction of an Antarctic tardigrade retrieved from a moss sample frozen for over 30 years. *Cryobiology* **72**, 78–81 (2016).
11. Kagoshima, H. *et al.* Multi-decadal survival of an Antarctic nematode, Plectus murrayi, in a -20°C stored moss sample. *CryoLetters* **33**, 280–288 (2012).
12. Steiner, G. & Florence E, A. Resuscitation of the nematode Tylenchus polyhypnus, n. sp., after almost 39 years' dormancy. *J. Wash. Acad. Sci.* **36**, 97–99.
13. Gilichinsky, D. A. *et al.* Microbial Populations in Antarctic Permafrost: Biodiversity, State, Age, and Implication for Astrobiology. *Astrobiology* **7**, 275–311 (2007).
14. Rivkina, E. *et al.* Earth's perennially frozen environments as a model of cryogenic planet ecosystems. *Permafr. Periglac. Process.* **29**, 246–256 (2018).

660 15.Sipes, K. *et al.* Eight Metagenome-Assembled Genomes Provide Evidence for Microbial
661 Adaptation in 20,000- to 1,000,000-Year-Old Siberian Permafrost. *Appl. Environ.*
662 *Microbiol.* **87**, (2021).
663 16.Liang, R. *et al.* Genomic reconstruction of fossil and living microorganisms in ancient
664 Siberian permafrost. *Microbiome* **9**, 110 (2021).
665 17.Gilichinsky, D. A. & Rivkina, E. M. Permafrost Microbiology. 7 (2011).
666 18.Yashina, S. *et al.* Regeneration of whole fertile plants from 30,000-y-old fruit tissue buried
667 in Siberian permafrost. *Proc. Natl. Acad. Sci.* **109**, 4008–4013 (2012).
668 19.Adhikari, B. N., Wall, D. H. & Adams, B. J. Desiccation survival in an Antarctic nematode:
669 molecular analysis using expressed sequenced tags. *BMC Genomics* **10**, 69 (2009).
670 20.Tyson, T. *et al.* A molecular analysis of desiccation tolerance mechanisms in the
671 anhydrobiotic nematode Panagrolaimus superbus using expressed sequenced tags. *BMC*
672 *Res. Notes* **5**, 68 (2012).
673 21.McGill, L. M. *et al.* Anhydrobiosis and Freezing-Tolerance: Adaptations That Facilitate the
674 Establishment of Panagrolaimus Nematodes in Polar Habitats. *PLOS ONE* **10**, e0116084
675 (2015).
676 22.Thorne, M. A. S., Kagoshima, H., Clark, M. S., Marshall, C. J. & Wharton, D. A. Molecular
677 Analysis of the Cold Tolerant Antarctic Nematode, Panagrolaimus davidi. *PLoS ONE* **9**,
678 e104526 (2014).
679 23.Sandhove, J., Spann, N. & Ristau, K. The Anhydrobiotic Potential of the Terrestrial
680 Nematodes *Plectus parietinus* and *Plectus velox*: Anhydrobiosis OF *Plectus parietinus* and
681 *P. velox*. *J. Exp. Zool. Part Ecol. Genet. Physiol.* **325**, 434–440 (2016).
682 24.Erkut, C. *et al.* Trehalose Renders the Dauer Larva of Caenorhabditis elegans Resistant to
683 Extreme Desiccation. *Curr. Biol.* **21**, 1331–1336 (2011).
684 25.Erkut, C., Gade, V. R., Laxman, S. & Kurzchalia, T. V. The glyoxylate shunt is essential
685 for desiccation tolerance in C. elegans and budding yeast. *elife* **5**, (2016).
686 26.Zanina, O. G., Gubin, S. V., Kuzmina, S. A., Maximovich, S. V. & Lopatina, D. A. Late-
687 Pleistocene (MIS 3-2) palaeoenvironments as recorded by sediments, palaeosols, and
688 ground-squirrel nests at Duvanny Yar, Kolyma lowland, northeast Siberia. *Quat. Sci. Rev.*
689 **30**, 2107–2123 (2011).
690 27.Murton, J. B. *et al.* Palaeoenvironmental Interpretation of Yedoma Silt (Ice Complex)
691 Deposition as Cold-Climate Loess, Duvanny Yar, Northeast Siberia: Palaeoenvironmental

692 Interpretation of Yedoma Silt, Duvanny Yar. *Permafr. Periglac. Process.* **26**, 208–288
693 (2015).
694 28.Abramov, A., Vishnivetskaya, T. & Rivkina, E. Are permafrost microorganisms as old as
695 permafrost? *FEMS Microbiol. Ecol.* **97**, fiaa260 (2021).
696 29.Gilichinsky, D. A., Wagener, S. & Vishnevetskaya, T. A. Permafrost microbiology.
697 *Permafr. Periglac. Process.* **6**, 281–291 (1995).
698 30.Schiffer, P. H. *et al.* Signatures of the Evolution of Parthenogenesis and Cryptobiosis in the
699 Genomes of Panagrolaimid Nematodes. *iScience* **21**, 587–602 (2019).
700 31.Schiffer, P. H. *et al.* Developmental variations among Panagrolaimid nematodes indicate
701 developmental system drift within a small taxonomic unit. *Dev. Genes Evol.* **224**, 183–188
702 (2014).
703 32.Dey, A., Chan, C. K. W., Thomas, C. G. & Cutter, A. D. Molecular hyperdiversity defines
704 populations of the nematode Caenorhabditis brenneri. *Proc. Natl. Acad. Sci.* **110**, 11056–
705 11060 (2013).
706 33.Cutter, A. D. Divergence Times in Caenorhabditis and Drosophila Inferred from Direct
707 Estimates of the Neutral Mutation Rate. *Mol. Biol. Evol.* **25**, 778–786 (2008).
708 34.Seybold, A. C., Wharton, D. A., Thorne, M. A. S. & Marshall, C. J. Investigating trehalose
709 synthesis genes after cold acclimation in the Antarctic nematode *Panagrolaimus* sp. DAW1.
710 *Biol. Open* bio.023341 (2017) doi:10.1242/bio.023341.
711 35.Evangelista, C. C. S. *et al.* Multiple genes contribute to anhydrobiosis (tolerance to extreme
712 desiccation) in the nematode Panagrolaimus superbus. *Genet. Mol. Biol.* **40**, 790–802
713 (2017).
714 36.Malavin, S., Shmakova, L., Claverie, J.-M. & Rivkina, E. Frozen Zoo: a collection of
715 permafrost samples containing viable protists and their viruses. *Biodivers. Data J.* **8**, e51586
716 (2020).
717 37.Krivushin, K. *et al.* Two Metagenomes from Late Pleistocene Northeast Siberian
718 Permafrost. *Genome Announc.* **3**, e01380-14 (2015).
719 38.Zhou, J. *et al.* Phylogenetic diversity of a bacterial community determined from Siberian
720 tundra soil DNA. *Microbiology* **143**, 3913–3919 (1997).
721 39.Kapterev, P. Anabiosis in the conditions of permanent congelation. *Izv Akad Nauk SSSR Ser*
722 *Biol* **6**, 1073–1088 (1936).
723 40.Kapterev, P. New data on revitalization of organisms from perpetually frozen grounds. *CR*
724 *Acad Sci URSS* **20**, 315–317 (1938).

725 41.Andrássy, I. *Klasse Nematoda*. (Gustav Fischer Verlag, 1984).
726 42.Lewis, S. C. *et al.* Molecular evolution in Panagrolaimus nematodes: origins of
727 parthenogenesis, hermaphroditism and the Antarctic species P. davidi. *BMC Evol. Biol.* **9**,
728 15 (2009).
729 43.Andrássy, I. *Free-living Nematodes of Hungary*. (Hungarian Natural History Museum,
730 2005).
731 44.Schulenburg, H. & Félix, M.-A. The Natural Biotic Environment of *Caenorhabditis*
732 *elegans*. *Genetics* **206**, 55–86 (2017).
733 45.Frézal, L. & Félix, M.-A. C. elegans outside the Petri dish. *eLife* **4**, e05849 (2015).
734 46.Gems, D. *et al.* Two pleiotropic classes of daf-2 mutation affect larval arrest, adult behavior,
735 reproduction, and longevity in Caenorhabditis elegans. *Genetics* **150**, 129–155 (1998).
736 47.Vowels, J. J. & Thomas, J. H. Multiple chemosensory defects in daf-11 and daf-21 mutants
737 of Caenorhabditis elegans. *Genetics* **138**, 303–316 (1994).
738 48.Ren Peifeng *et al.* Control of C. elegans Larval Development by Neuronal Expression of a
739 TGF-β Homolog. *Science* **274**, 1389–1391 (1996).
740 49.Gerisch, B., Weitzel, C., Kober-Eisermann, C., Rottiers, V. & Antebi, A. A Hormonal
741 Signaling Pathway Influencing C. elegans Metabolism, Reproductive Development, and
742 Life Span. *Dev. Cell* **1**, 841–851 (2001).
743 50.Penkov, S. *et al.* Integration of carbohydrate metabolism and redox state controls dauer
744 larva formation in Caenorhabditis elegans. *Nat. Commun.* **6**, 8060 (2015).
745 51.Penkov, S. *et al.* A metabolic switch regulates the transition between growth and diapause
746 in C. elegans. *BMC Biol.* **18**, 31 (2020).
747 52.Nurk, S. *et al.* HiCanu: accurate assembly of segmental duplications, satellites, and allelic
748 variants from high-fidelity long reads. *Genome Res.* **30**, 1291–1305 (2020).
749 53.Laetsch, D. R. & Blaxter, M. L. BlobTools: Interrogation of genome assemblies.
750 *F1000Research* **6**, 1287 (2017).
751 54.Brůna, T., Hoff, K. J., Lomsadze, A., Stanke, M. & Borodovsky, M. BRAKER2: automatic
752 eukaryotic genome annotation with GeneMark-EP+ and AUGUSTUS supported by a
753 protein database. *NAR Genomics Bioinforma.* **3**, lqaa108 (2021).
754 55.Smythe, A. B., Holovachov, O. & Kocot, K. M. Improved phylogenomic sampling of free-
755 living nematodes enhances resolution of higher-level nematode phylogeny. *BMC Evol. Biol.*
756 **19**, 121 (2019).

757 56.Ahmed, M., Adedidran, F. & Holovachov, O. A draft transcriptome of a parasite
758 Neocamacolaimus parasiticus (Camacolaimidae, Plectida). *J. Nematol.* **53**, 1–4 (2021).
759 57.Grabherr, M. G. *et al.* Full-length transcriptome assembly from RNA-Seq data without a
760 reference genome. *Nat. Biotechnol.* **29**, 644–652 (2011).
761 58.Goecks, J., Nekrutenko, A., Taylor, J. & Galaxy Team, T. Galaxy: a comprehensive
762 approach for supporting accessible, reproducible, and transparent computational research in
763 the life sciences. *Genome Biol.* **11**, R86 (2010).
764 59.Haas, B. J. *et al.* De novo transcript sequence reconstruction from RNA-seq using the
765 Trinity platform for reference generation and analysis. *Nat. Protoc.* **8**, 1494–1512 (2013).
766 60.Li, W. & Godzik, A. Cd-hit: a fast program for clustering and comparing large sets of
767 protein or nucleotide sequences. *Bioinformatics* **22**, 1658–1659 (2006).
768 61.Fu, L., Niu, B., Zhu, Z., Wu, S. & Li, W. CD-HIT: accelerated for clustering the next-
769 generation sequencing data. *Bioinformatics* **28**, 3150–3152 (2012).
770 62.Emms, D. M. & Kelly, S. OrthoFinder: solving fundamental biases in whole genome
771 comparisons dramatically improves orthogroup inference accuracy. *Genome Biol.* **16**, 157
772 (2015).
773 63.Emms, D. M. & Kelly, S. OrthoFinder: phylogenetic orthology inference for comparative
774 genomics. *Genome Biol.* **20**, 238 (2019).
775 64.Katoh, K. & Standley, D. M. MAFFT Multiple Sequence Alignment Software Version 7:
776 Improvements in Performance and Usability. *Mol. Biol. Evol.* **30**, 772–780 (2013).
777 65.Capella-Gutierrez, S., Silla-Martinez, J. M. & Gabaldon, T. trimAl: a tool for automated
778 alignment trimming in large-scale phylogenetic analyses. *Bioinformatics* **25**, 1972–1973
779 (2009).
780 66.Minh, B. Q. *et al.* IQ-TREE 2: New Models and Efficient Methods for Phylogenetic
781 Inference in the Genomic Era. *Mol. Biol. Evol.* **37**, 1530–1534 (2020).
782 67.Jones, P. *et al.* InterProScan 5: genome-scale protein function classification. *Bioinformatics*
783 **30**, 1236–1240 (2014).
784 68.Huson, D. H. & Scornavacca, C. Dendroscope 3: An Interactive Tool for Rooted
785 Phylogenetic Trees and Networks. *Syst. Biol.* **61**, 1061–1067 (2012).
786 69.Kück, P. & Meusemann, K. FASconCAT: Convenient handling of data matrices. *Mol.*
787 *Phylogenet. Evol.* **56**, 1115–1118 (2010).

70. Nguyen, L.-T., Schmidt, H. A., von Haeseler, A. & Minh, B. Q. IQ-TREE: A Fast and Effective Stochastic Algorithm for Estimating Maximum-Likelihood Phylogenies. *Mol. Biol. Evol.* **32**, 268–274 (2015).
71. Kalyaanamoorthy, S., Minh, B. Q., Wong, T. K. F., von Haeseler, A. & Jermiin, L. S. ModelFinder: fast model selection for accurate phylogenetic estimates. *Nat. Methods* **14**, 587–589 (2017).
72. Zhang, C., Scornavacca, C., Molloy, E. K. & Mirarab, S. ASTRAL-Pro: Quartet-Based Species-Tree Inference despite Paralogy. *Mol. Biol. Evol.* **37**, 3292–3307 (2020).
73. Ranallo-Benavidez, T. R., Jaron, K. S. & Schatz, M. C. GenomeScope 2.0 and Smudgeplot for reference-free profiling of polyploid genomes. *Nat. Commun.* **11**, 1432 (2020).
74. Kokot, M., Długosz, M. & Deorowicz, S. KMC 3: counting and manipulating k-mer statistics. *Bioinformatics* **33**, 2759–2761 (2017).
75. Thomas, GWC., Ather, H. S., Hahn, W. Matthew. Gene-Tree Reconciliation with MUL-Trees to Resolve Polyploidy Events. Systematic Biology 66, 1007-1018 (2017).

Figure legends

Figure 1. Study site.

a) location of the Duvanny Yar outcrope on the Kolyma River, northeastern Siberia, Russia. b) view of the upper part of outcrop composed of ice wedges and permafrost silty deposits. c) lithostratigraphic scheme of deposits, showing location of studied rodent borrow (red circle). d) fossil rodent burrow with herbaceous litter and seeds buried in permafrost deposits; m a.r.l. = meters above river level.

Figure 2. General morphology of *Panagrolaimus n. sp*., female.

Scanning electron pictures (a, c), light microscopy photographs (e, f) and graphic presentations (b, d, g) of holotype: a, b) entire body, c, d) anterior ends, e) anterior body, f) perivulvar body region, g) tail. Abbreviations: l.f. – lateral field, ov – ovary, pro – procorpus of the pharynx, t.b. – terminal bulb of the pharynx, u – uterus with eggs, v – vulva, v.p. – ventral pore. Scale bars: a, d, e, f, g – 20 µm, b – 100 µm, c – 2 µm.

887 **Figure 3. Genome assembly and phylogenomics reveals that the newly discovered**
888 ***Panagrolaimus n. sp* species is triploid.**
889 a) Kmer spectra of the *Panagrolaimus n. sp* PacBio HiFi data. Kmers of length 19 were counted
890 using Jellyfish. b) Circos plot showing the triploid structure of the *Panagrolaimus n. sp*
891 genome. Lines represent the position of 6,715 homeologs in eight contigs that comprise 39.9
892 Mb (15%) of the assembly. Homeologs were identified by clustering protein-coding genes into
893 orthogroups using OrthoFinder and selecting groups containing three sequences. Contig IDs
894 and scale is shown. c) Inferred species tree for all taxa. The maximum likelihood tree inferred
895 using a concatenated supermatrix (18S and 28S genes) with bootstrap support values is
896 displayed. All genera are represented as monophyletic clades. *Panagrolaimus n. sp* is
897 highlighted in red and basal to all other *Panagrolaimus* taxa. Internal nodes, where all
898 subsequent branches represent identical sequences, are displayed with a black star. d)
899 *Panagrolaimus n. sp.* possesses *C. elegans* gene orthologs to enzymes required for TCA cycle,
900 glyoxylate shunt, glycolysis, gluconeogenesis, trehalose synthesis, and polyamine synthesis.
901 Black filled circles: Ortholog presence suggested by orthogroup clustering, phylogenetic
902 analysis, and domain architecture. White filled circles: No ortholog found via current analysis.
903 Coloured filled circles: Presence of *Panagrolaimus n. sp.* gene(s), related to several *C. elegans*
904 genes (all genes of same colour) that are all co-orthologous to that gene (those genes). Label:
905 *C. elegans* enzyme names and orthogroup that contains that gene according to our orthogroup
906 clustering.
907
908
909
910
911
912
913
914
915
916
917
918
919

920 **Figure 4. *C. elegans* dauer larvae and *Panagrolaimus n. sp.* might utilize similar**
921 **mechanisms to survive cryptobiosis.**
922 a) Survival rate of *Panagrolaimus n. sp.* nematodes to desiccation and freezing (-80°C). Error
923 bars indicate standard error of mean of two independent experiments with two technical
924 replicates performed on two different days. Statistical comparison was performed using
925 unpaired t test with Welch correction. n.s. $p > 0.05$, ****$p < 0.0001$. For desiccation (non-
926 preconditioned) n = 289, freezing (non-preconditioned) n = 675, desiccation (preconditioned
927 at 98%RH) n = 953 and freezing (preconditioned at 98%RH) n = 1295. b) *Panagrolaimus n.*
928 *sp.* nematodes and *daf-2(e1370)* dauer larvae upregulate trehalose levels upon preconditioning
929 at 98%RH. Error bars indicate standard error of mean of two independent experiments with
930 three replicates performed on two different days. Statistical comparison was performed using
931 two-way ANOVA with Holm-Sidak's multiple comparison test, ****$p < 0.0001$. c-d) 2D-thin
932 layer chromatography of ^{14}C-acetate labelled metabolites from *Panagrolaimus n. sp.* that were
933 non-preconditioned and preconditioned at 98%RH. Enumerated spots indicate trehalose (1),
934 glucose (2), glutamate (3), glutamine (4), serine/glycine (5) and phenylalanine (6).
935 Representative images from at least two independent experiments performed on two different
936 days. e) Desiccated *daf-2 (e1370)* dauer larvae survive to freezing (-80°C) for an extremely
937 long period. Error bars indicate standard error of mean of two independent experiments with
938 two technical replicates performed on two different days. f) Brood size of desiccated dauer
939 larvae exposed to freezing remain like that non- desiccated dauer larvae. Average brood size is
940 the mean of seven dauer larvae per each condition. Statistical comparison was performed by
941 using non-parametric Kolmogorov-smirnov test n.s $p>0.05$.
942
943
944
945
946
947
948
949
950
951
952

Figure S1. Calibration of a radiocarbon (^{14}C) date.

Radiocarbon date (44,315±405 BP) and calibrated age (45,839 -- 47,769 cal BP) of plant material collected from buried borrow P-1320. Radiocarbon ages were converted to calendar age equivalents with the OxCal V.4.4 program using the IntCal20 calibration curve. Pink-shaded area — radiocarbon date with standard deviation; grey-shaded area — radiocarbon date projection on the calibration curve with 95.4% probability.

Figure S2. Morphology of *Panagrolaimus n. sp* sp. n., female.

Graphic presentations of holotype (a,b) and SEM pictures (c-i): a) anterior body, b) female reproductive branch, c–e) anterior end of three different female specimens, f) anterior part of the lateral ridge, g) vulva, h) ventral excretory/secretory pore, i) posterior body with anus and lateral ridge. Scale bars: a,b - 50 µm, c,i - 3 µm, d - 2 µm, e –1 µm, f,h - 5 µm, g - 10 µm, .

1018 **Figure S3. Phylogenies inferred for genes sets using both concatenation and coalescence**
1019 **approaches.**
1020 a) The ploidy level was analysed with *Smudgeplot* v0.2.1[73]. KMC version 3.1.0[74] was used
1021 to count the 21-mers in the PacBio CCS reads. Then we ran *smudgeplot.py* to determine the
1022 lower and upper coverage cut-offs. These were determined to be 14 and 380. 21-mers with a
1023 coverage between 14 and 380 were filtered with kmc_tools. Then, we computed the k-mer
1024 pairs from the filtered 21-mers by running *smudgeplot.py hetkmers*. Finally, the produced a
1025 smudgeplot shows an estimated ploidy of 3. b) Species tree inferred for 12,295 gene trees using
1026 coalescence approach. The species tree implemented using the coalescence approach with
1027 orthogroup gene tree is displayed. Novel species in this study are displayed in red. All nodes
1028 have a posterior probability of 1. c) Species tree inferred for 102 taxa**.** The maximum likelihood
1029 tree inferred using a concatenated supermatrix of 60 genes is displayed. Bootstrap values are
1030 only displayed for nodes with less than 100% support. The platyhelminth *Macrostum lignano*
1031 serves as an outgroup for rooting. The ancestral *Panagrolaimus*, sister to all others within the
1032 *Panagrolaimus* genus, is highlighted in red.
1033
1034
1035
1036
1037
1038
1039
1040
1041
1042
1043
1044
1045
1046
1047
1048
1049

1050 **Figure S4. Combination of cryptobiotic states enhances survival of *C. elegans* dauer**
1051 **larvae.**
1052 a) Desiccated dauer larvae manifest enhanced survival rate to heat stress (34°C). Error bars
1053 indicate standard deviation of two independent experiments with two technical replicates. b)
1054 Desiccated dauer larvae display enhances survival rate to anoxia. Error bars indicate standard
1055 deviation of two independent experiments with two technical replicates. Statistical
1056 comparison was performed by paired two tailed t-test. *$p<0.05$. c) *Panagrolaimus n. sp.*
1057 possesses gene orthologs to most genes implicated in dauer formation and metabolism in *C.*
1058 *elegans*. Black filled circles: Ortholog presence suggested by orthogroup clustering,
1059 phylogenetic analysis, and domain architecture. White filled circles: No ortholog found via
1060 current analysis (in all cases these *C. elegans* genes did not cluster with any *Panagrolaimus*
1061 genes in the orthogroup clustering). Label: *C. elegans* enzyme names and orthogroup that
1062 contains that gene according to our orthogroup clustering.
1063
1064
1065
1066
1067
1068
1069
1070
1071
1072
1073
1074
1075
1076
1077
1078
1079
1080
1081
1082
1083

1084 **Figure S5. *Panagrolaimus n. sp.* reduces triacylglycerols (TAGs) levels and accumulates**
1085 **trehalose-6-phosphate upon preconditioning at 98%RH**.
1086 a) 1D-Thin layer chromatography of acetate labelled organic fractions of non-preconditioned
1087 (1) and preconditioned (2) *P. kolymaensis*. b) Mass spectrometric quantification of TAG levels
1088 of non-preconditioned (1) and preconditioned (2) *P. kolymaensis*. Error bars indicate standard
1089 deviation of two biological replicates with two technical replicates. Statistical analysis was
1090 performed using unpaired t-test with Welch correction **$p < 0.001$. c-d) non-preconditioned
1091 and preconditioned mass spectrum of an empty region, e-f) spot 1 (trehalose), g-h) spot 7
1092 (trehalose-6-phosphate) scraped out and extracted from the 2D-TLC.
1093
1094
1095
1096
1097
1098
1099
1100
1101
1102
1103
1104
1105
1106
1107
1108
1109
1110
1111
1112
1113
1114
1115
1116

1117 **Figure S6. Exploring a possible allopolyploid origin for extra proteins.**

1118 Gene-tree reconciliation was used to determine whether extra sets of proteins across
1119 orthogroups originate through auto- or allopolyploidy. Different copies of proteins (designated
1120 by '+' and '*') suggest an allopolyploid origin. Parthenogenetic species are highlighted in bold.

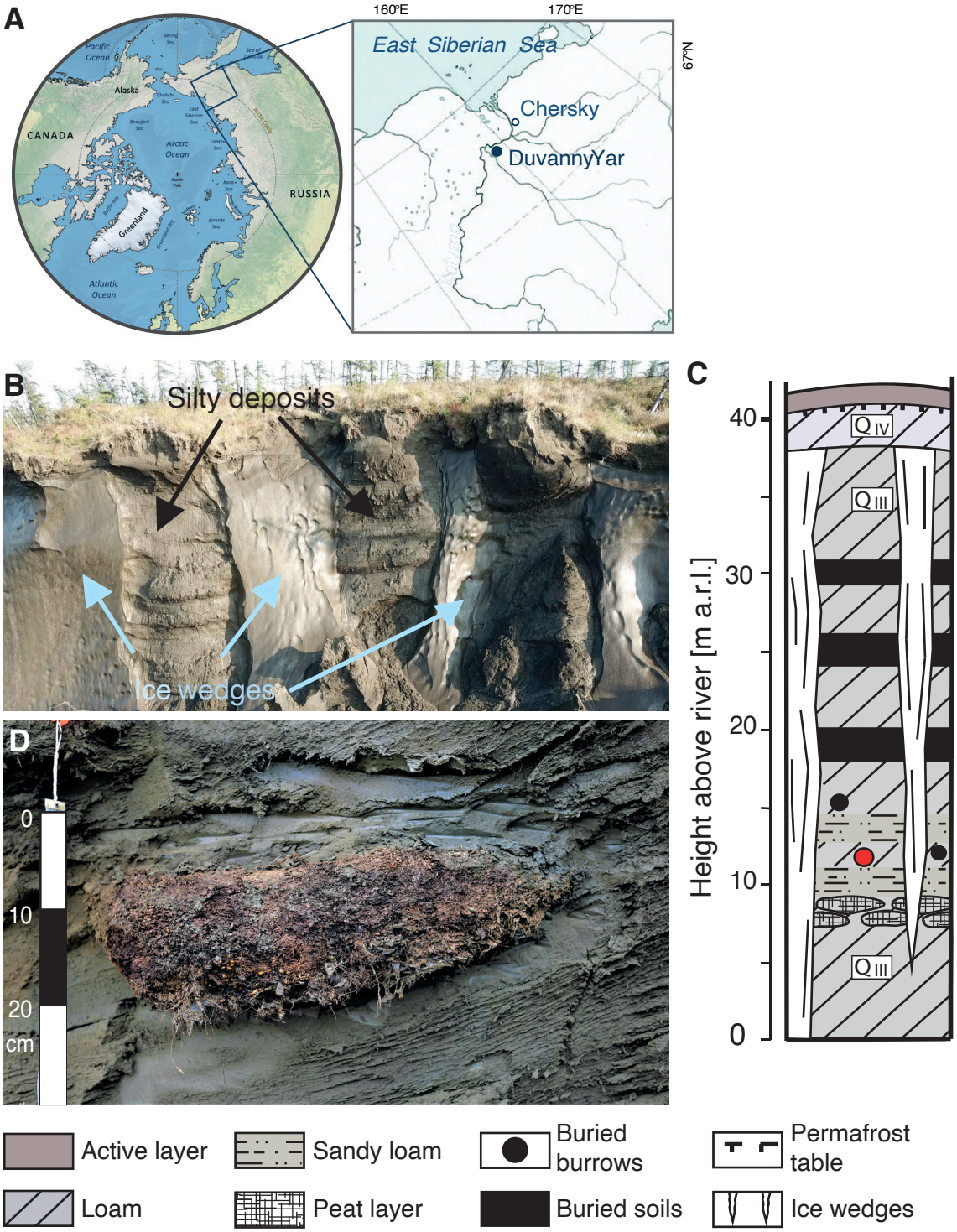

Figure 1
Shatilovich *et al*

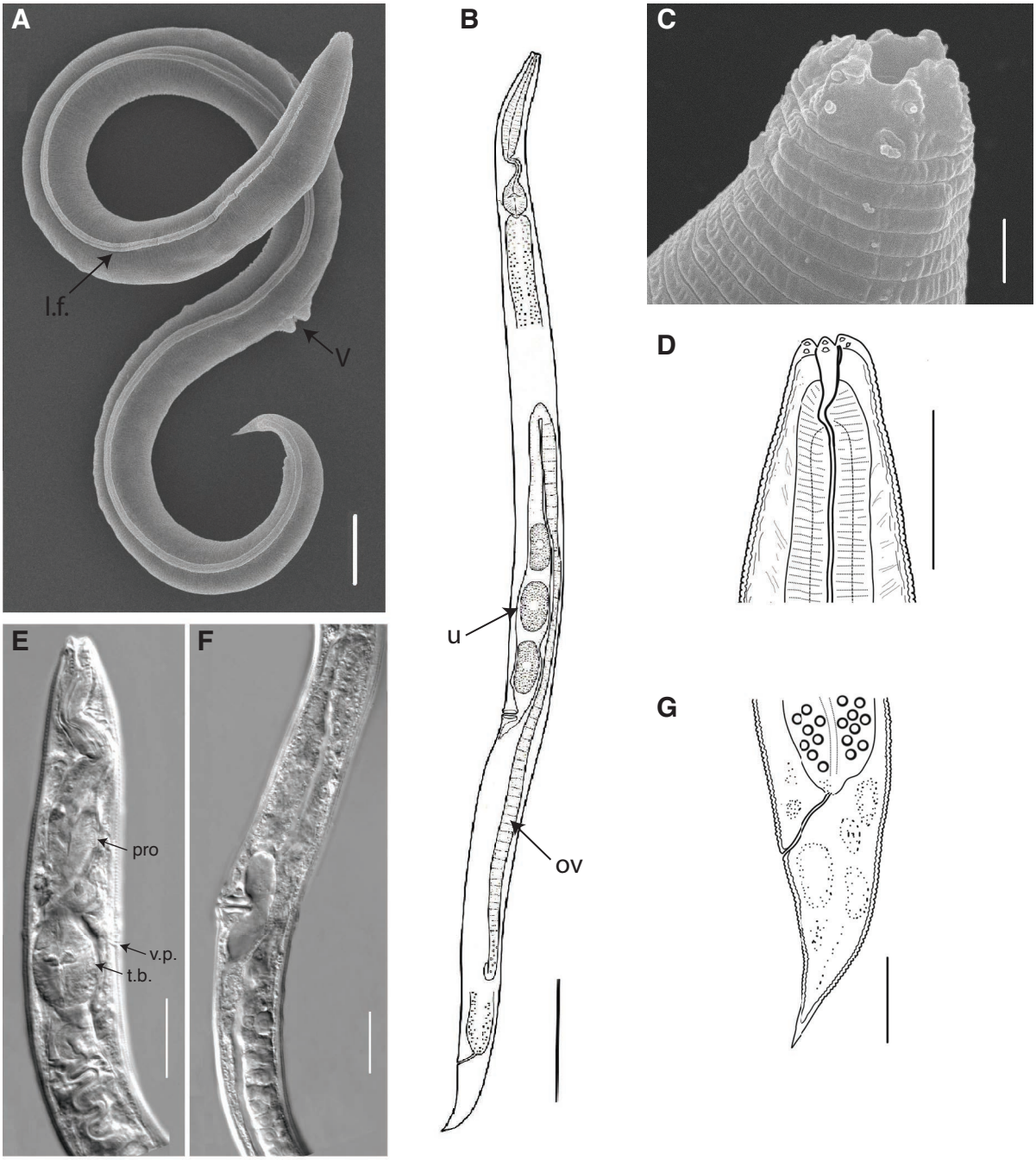

Figure 2
Shatilovich *et al*

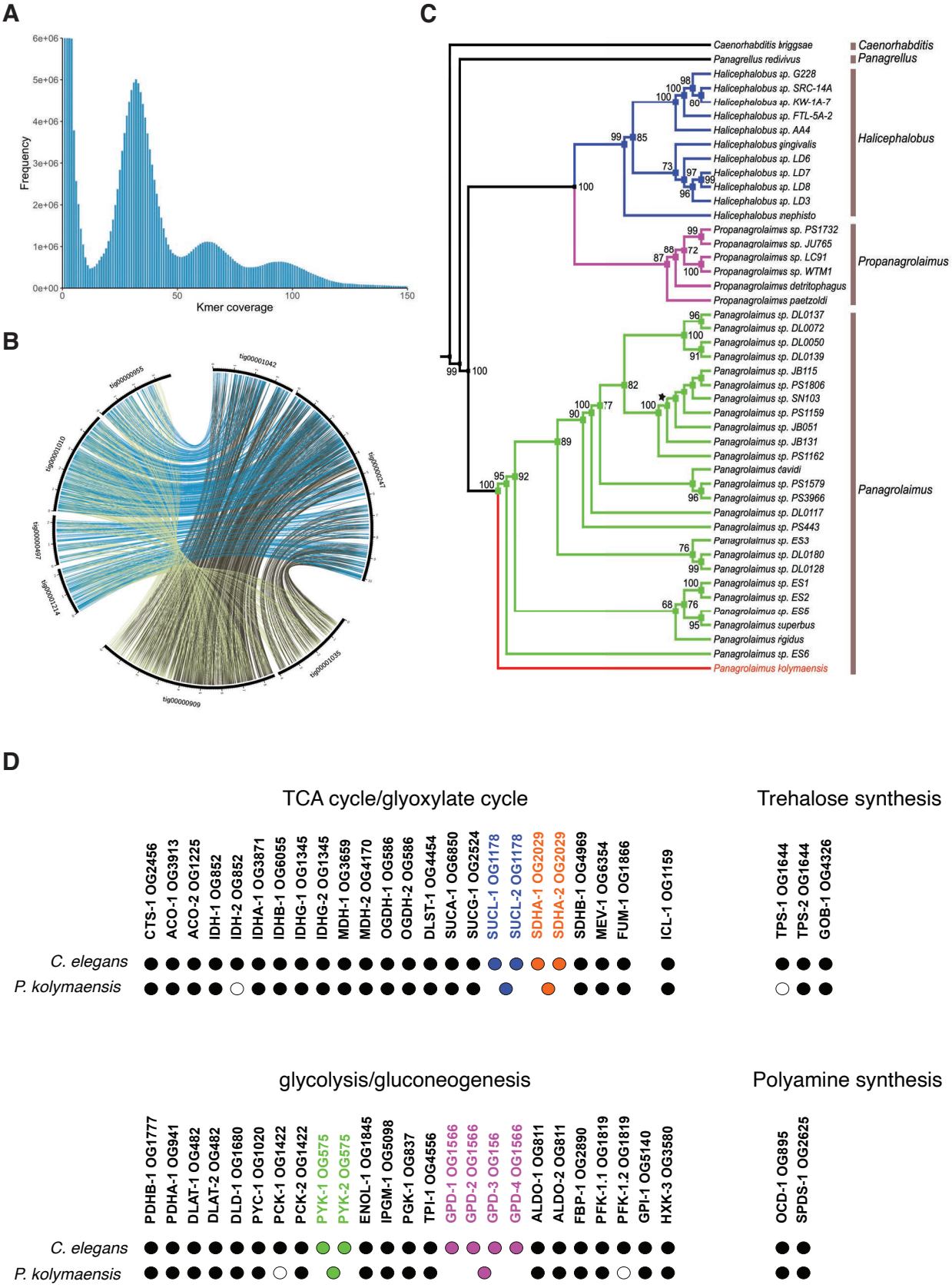

Figure 3
Shatilovich *et al*

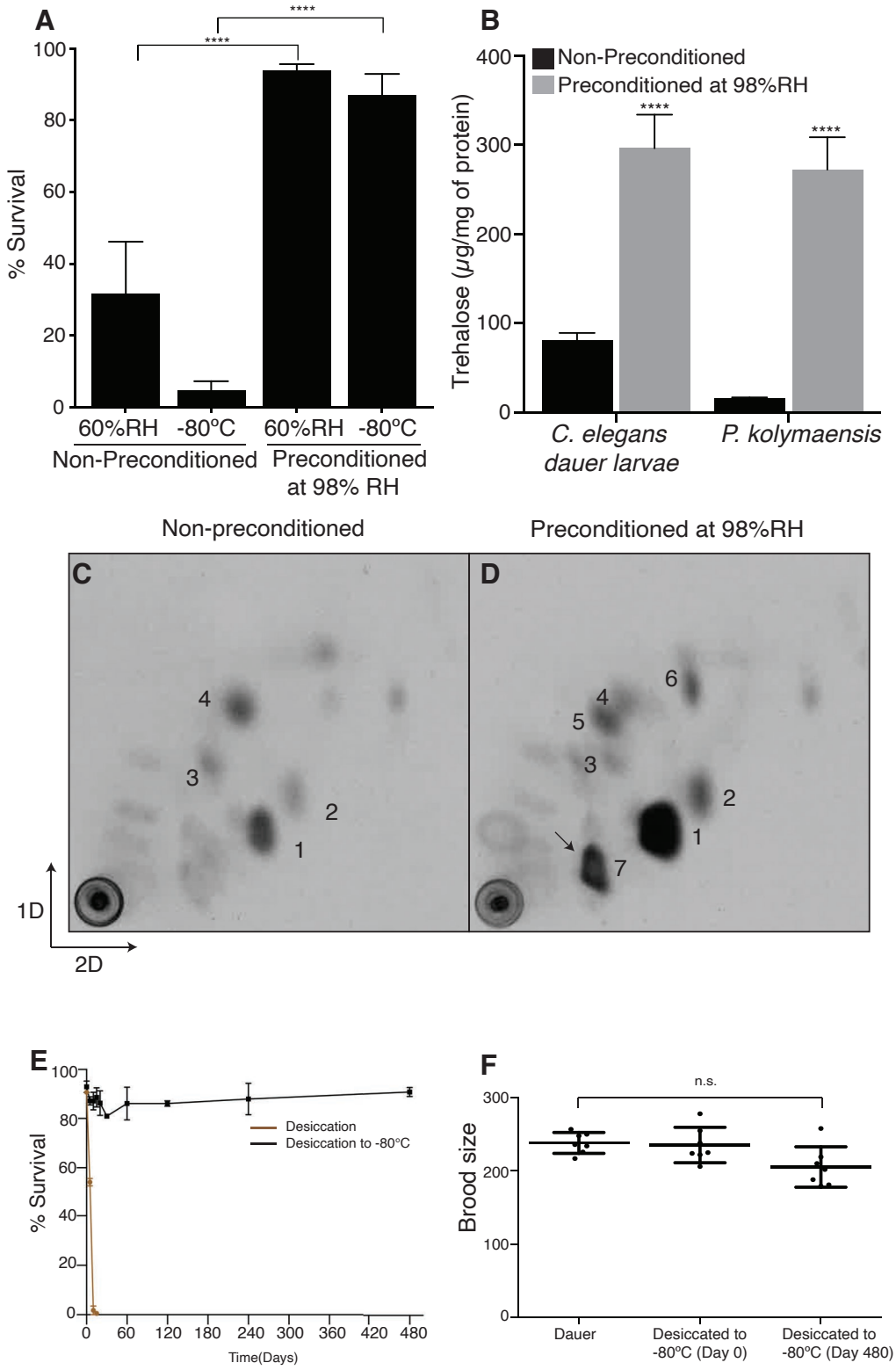

Figure 4
Shatilovich *et al*

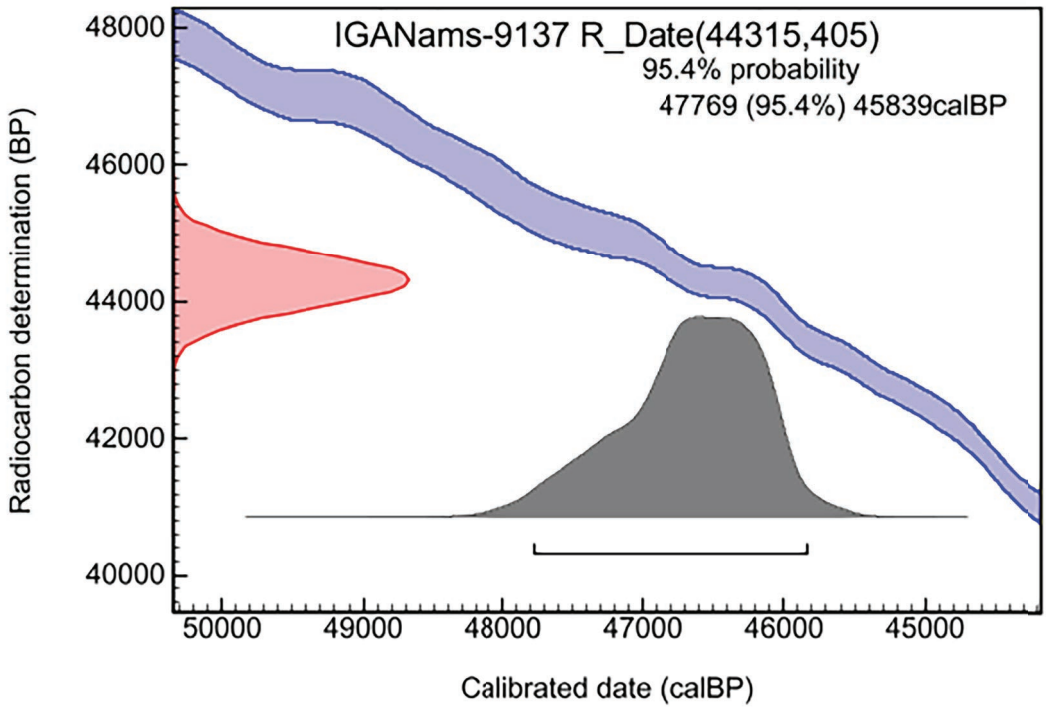

Figure S1
Shatilovich *et al*

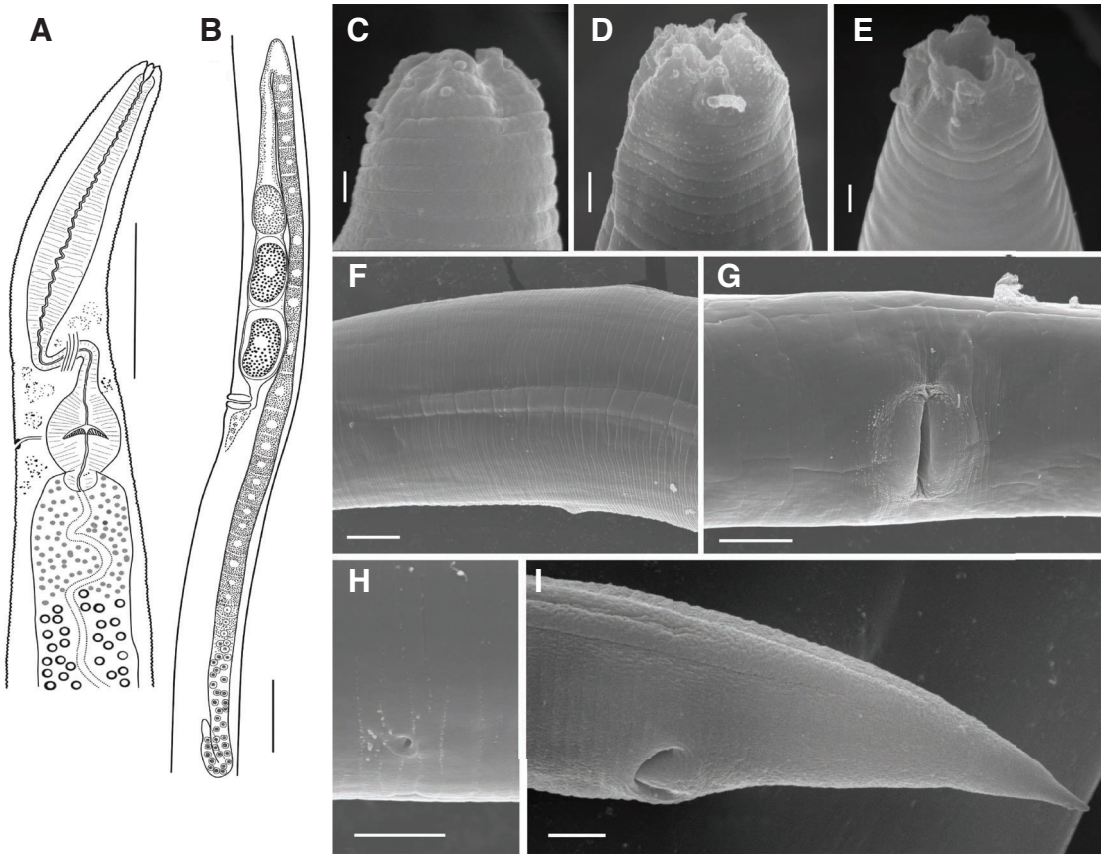

Figure S2
Shatilovich *et al*

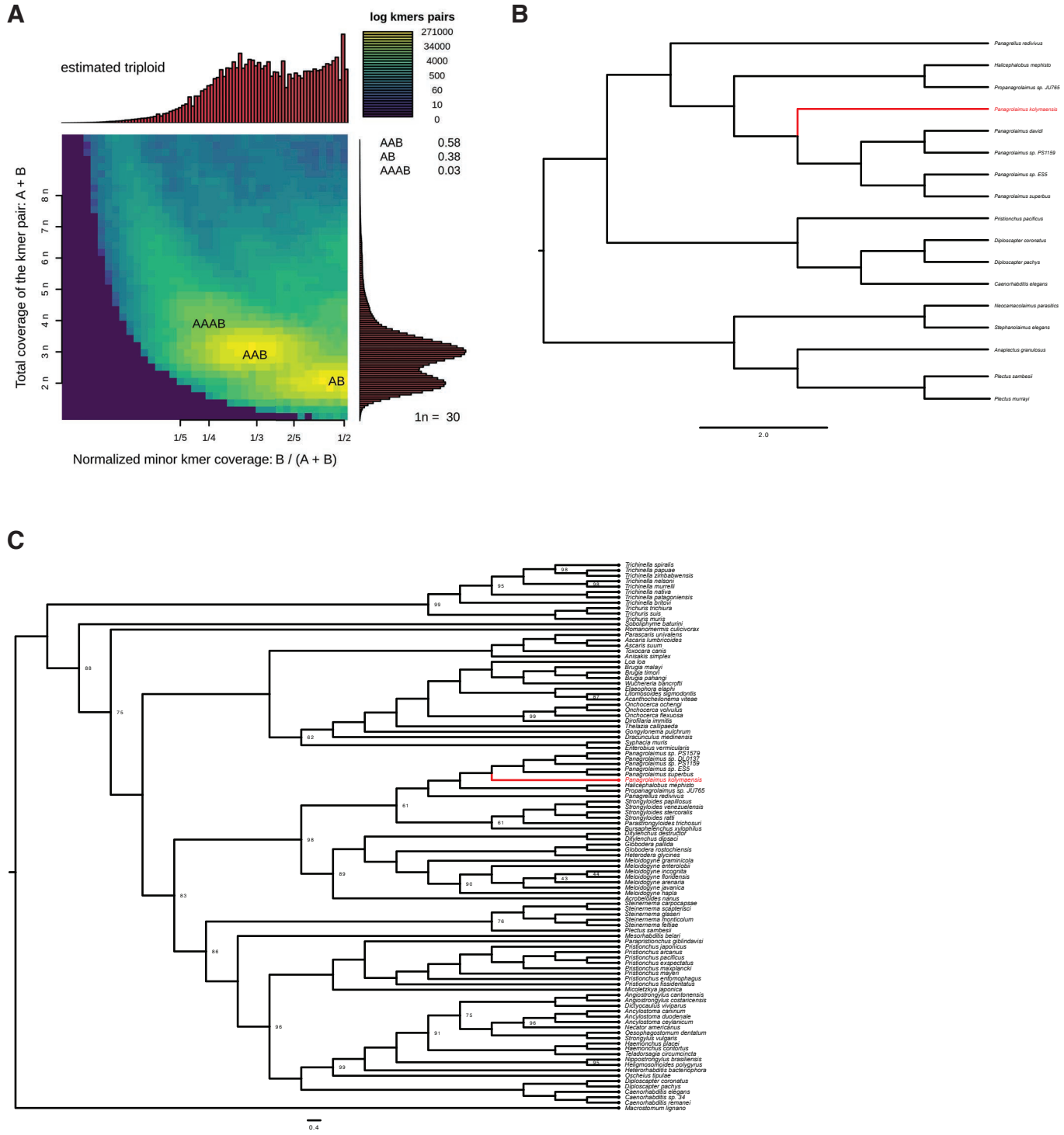

Figure S3
Shatilovich *et al*

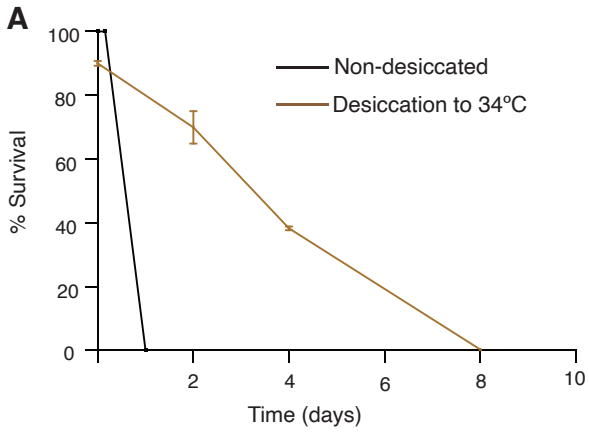

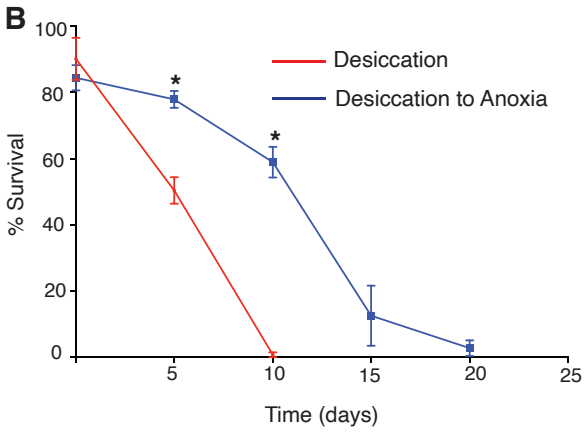

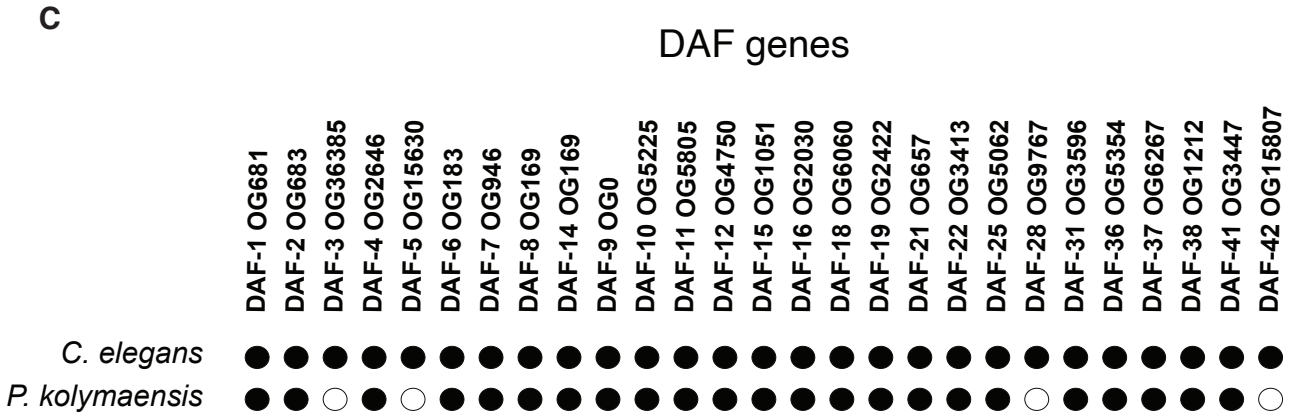

Figure S4
Shatilovich *et al*

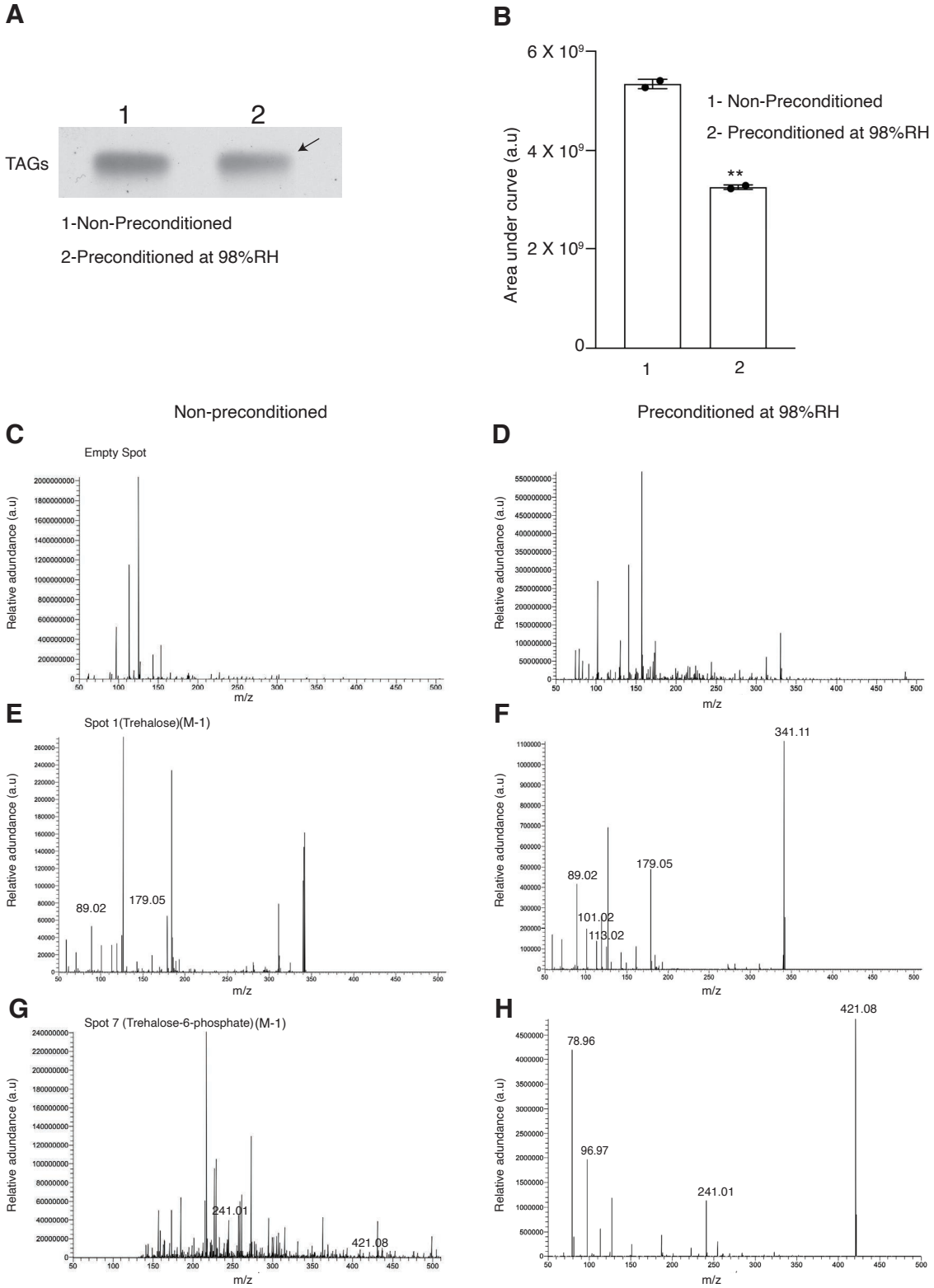

Figure S5
Shatilovich *et al*

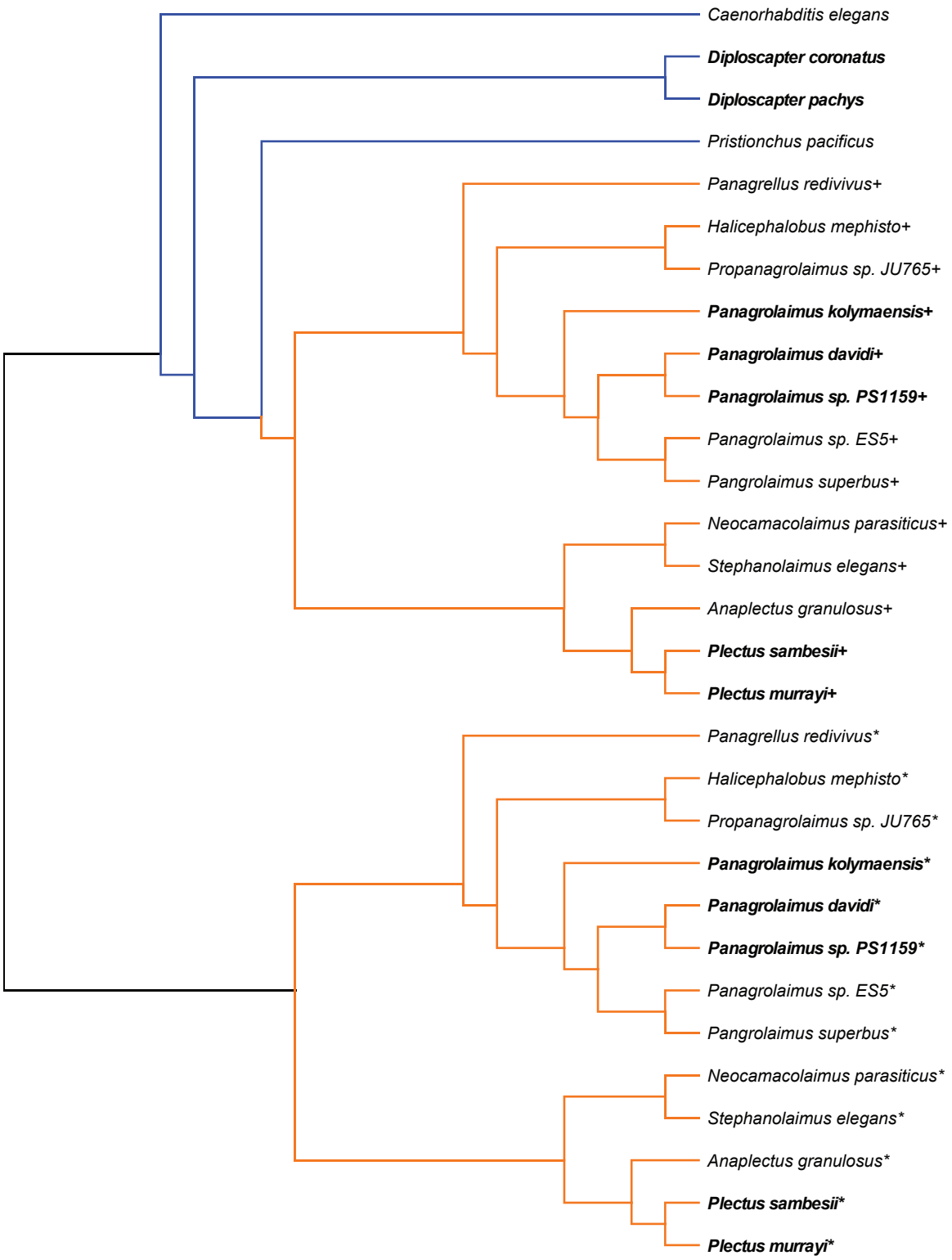

Figure S6
Shatilovich *et al*